# Quasi-static compression tests of overwrapped composite pressure vessels under low velocity impact.

MOHAMMED, A.I., RAGHUPATHY, K., BALTAZAR, O.D.V.G., ONOKPASAH, L., CARVALHO, R., MOGENSEN, A., HASSANI, F. and NJUGUNA, J.

2023

Composite Structures 327 (2024) 117662

Contents lists available at ScienceDirect

Composite Structures

journal homepage: www.elsevier.com/locate/compstruct

# Quasi-static compression tests of overwrapped composite pressure vessels under low velocity impact

Auwalu I. Mohammed [a], Kaarthikeyan Raghupathy [a], Osvaldo De Victoria Garcia Baltazar [a], Lawson Onokpasah [b], Roger Carvalho [b], Anders Mogensen [b], Farzaneh Hassani [a], James Njuguna [a,*]

[a] School of Engineering, Robert Gordon University, Garthdee Road, Aberdeen, United Kingdom
[b] Dolphitech Limited, Milton Hally, Ely Road, Cambridge, United Kingdom

ARTICLE INFO

*Keywords:*
Composite
NDT
Damage
Pressure vessel
Compression
Hydrogen

ABSTRACT

Pressure vessels are being utilised in different applications that are indispensable including automobile, aerospace, underwater vehicles, oil and gas, chemical engineering among other applications. However, there is lack of knowledge on the influence of induced damage and the resulting performance of such vessels under quasi-static loading and axial compression. Specifically, the vessels studied in this study is made up of a high-density polyethylene liner and glass fibre overwraps. Therefore, this research investigated the load bearing capacities and the energy absorbed of the indented vessels in axial and hoop directions to determine the resistance of the vessels after such damaged using experiment, and damage characterisation microscopy, non-destructive testing and analysis.

Quasi-static transverse and axial compression testing was performed on composite cylinders made of polyethylene liner and glass fibre overwraps. Both quasi-static and axial compression tests were performed with Universal testing Machines at crosshead speed of 500 mm/min 2.5 mm/min respectively. Microstructural damage characterisation was conducted using microscopy and Dolphicam2 ultrasonic non-destructive testing equipment.

This study provides a new understanding on the performance of composite pressure vessel under damaged and undamaged conditions has established the reliability and residual strength capabilities of composites under the scenarios investigated. The results shows that the damage profile and the effect on compressive strength of the composite damaged and non-damaged cylinders was found to be relatively similar. However, when the cylinders are subjected to quasi-static compression, the polyethylene absorbs enough elastic strain energy to recover from the applied compressive load and recover without being plastically deformed. Additionally, the results demonstrate that the quasi-static compression have little or no influence on the axial strength of the cylinders. The damage characterisation on the cylinders revealed fibre break and delamination and local bucking and brooming failure at the bottom of the cylinders. This study has direct impact in composite overwrapped pressure vessels (COPVs) safety design tolerances, manufactururing strategy and operational failure conditions.

## 1. Introduction

Composite overwrapped pressure vessels (COPVs) are used in many industries such as defence, civil, automobile, oil and gas and aerospace applications [1,2]. These vessels exhibit excellent impact and fatigue resistance, high corrosion resistance and high stiffness/strength-to-weight ratio. Four different types of COPVs are distinguished and used in industry based on their applications and performance requirements. Type I vessels are fully metallic containers, while types II, III and IV are made of two layers; an internal liner which contains the liquid or pressurised gas, and the overwrapped high strength fibre around the liner to provide reinforcement. The liner is usually a thin metal or a thermoplastic polymer and act as the fluid impermeable layer and the overwrapped high strength fibre protects the liner from outside damages and bear the structural loads [3]. Several studies on composites pressure vessels have been published in the literature addressing different aspect

* Corresponding author.
*E-mail address:* j.njuguna@rgu.ac.uk (J. Njuguna).

https://doi.org/10.1016/j.compstruct.2023.117662
Received 2 June 2023; Received in revised form 16 October 2023; Accepted 26 October 2023
Available online 29 October 2023

**Table 1**
Vessels dimension and history/comments.

| Number of vessels | Outer Diameter (mm) | Inner Diameter (mm) | Length (mm) | Fibre Orientation | History/ Comments |
|---|---|---|---|---|---|
| 4 | 155 | 147 | 450.2 | 90°, ±45° | Previously indented and compressed |
| 2 | 152.4 | 114.5 | 457.2 | 90°, ±45° | No indentation |
| 2 | 155 | 147 | 147 and 162 | 90°, ±45° | Round cut tubes |

**Table 2**
Selected properties of glass fibre and hdpe liner.

| **Glass Fibre** | | |
|---|---|---|
| Property | Values | Units |
| Longitudinal strength | 800 | MPa |
| Longitudinal Modulus | 40 | GPa |
| Transverse Strength | 40 | MPa |
| Transverse Modulus | 10 | GPa |
| Shear strength | 35 | MPa |
| Shear Modulus | 0.5 | GPa |
| Poisson's ratio | 0.35 | – |
| Density | 1.9 | g/cm$^3$ |
| Glass Mass content | 70 | % |
| Glass volume content | 52 | % |
| **Liner** | | |
| Tensile modulus | 270 ± 8 | MPa |
| Yield stress | 13.8 ± 0.4 | MPa |
| Yield strain | 14.36 ± 0.4 | % |
| Elongation at break | >40 | % |
| Density | 0.94 | g/cm$^3$ |

of the vessel ranging from design to eventual decommissioning of the vessel.

For example, the study of Kangal et al. [4] analysed the damage mechanism of carbon fibre overwrapped composite vessels subjected to impact loads using flat, conical and hemispherical nose impactors. In the study of Wu et al. [5] examined the impact response of glass fibre overwrapped composite vessels through experiment. Also, Parillo et al. [6] quantify the residual burst strength of composite vessel after mechanical impacts and established a relationship between burst pressure and the incident energy. The study of Blanc-Vannet [7] on the effect of impact and compression after impact response of single stiffened composite specimen revealed that the fillers enhance the load bearing capacity and increase the damage tolerance.

The theoretical study of pressure vessel failure under low velocity impact and internal pressure by Zhang et al. [8] observed sequence of in-plane failure and delamination varies with increase in impact energy. Furthermore, in a similar study, Rafiee et al. [9,10], Azom [11], Ioneos [12] and Benham et al. [13] developed a theoretical model for the prediction of induced failure on composites subjected to low velocity impact. Besides, Sachse et al. [14] and Sutherland and Soares [15] study on quasi static tests to determine the static and dynamic impact behaviour of GRP composites found sudden appearance of an internal delamination at very low incident energy/displacement, followed by fibre failure at much higher incident energy/displacement. Krishnaswamy [16] and Curtis et al. [17] established that higher energy indentation caused buckling in composites tubes and reduced burst strength by 60 %. Meanwhile, the study of Korsunsky [18] and Zhang et al. [8] validated the modelling of a layered composite for improved accuracy in predicting low velocity impact damage. Weirdie and Lagace [15,19]

**Table 3**
Presents the pressure vessels samples, geometry and liner properties and test loads.

| Impact | Type /configuration | Materials | Liner | Testing load/speed |
|---|---|---|---|---|
| Impacted Pressure vessels | Transverse/ hoop | Glass Fibre | HDPE | 2.5 mm/ min |
| No impact | NA | Glass Fibre | HDPE | 2.5 mm/ min |
| Compressed Pressure vessels | Axial | Glass Fibre | HDPE | 500 mm/ min |
| Quasi- Static compressed Pressure vessels | Quasi-Static Compression | Glass Fibre | HDPE | 2.5 mm/ min |

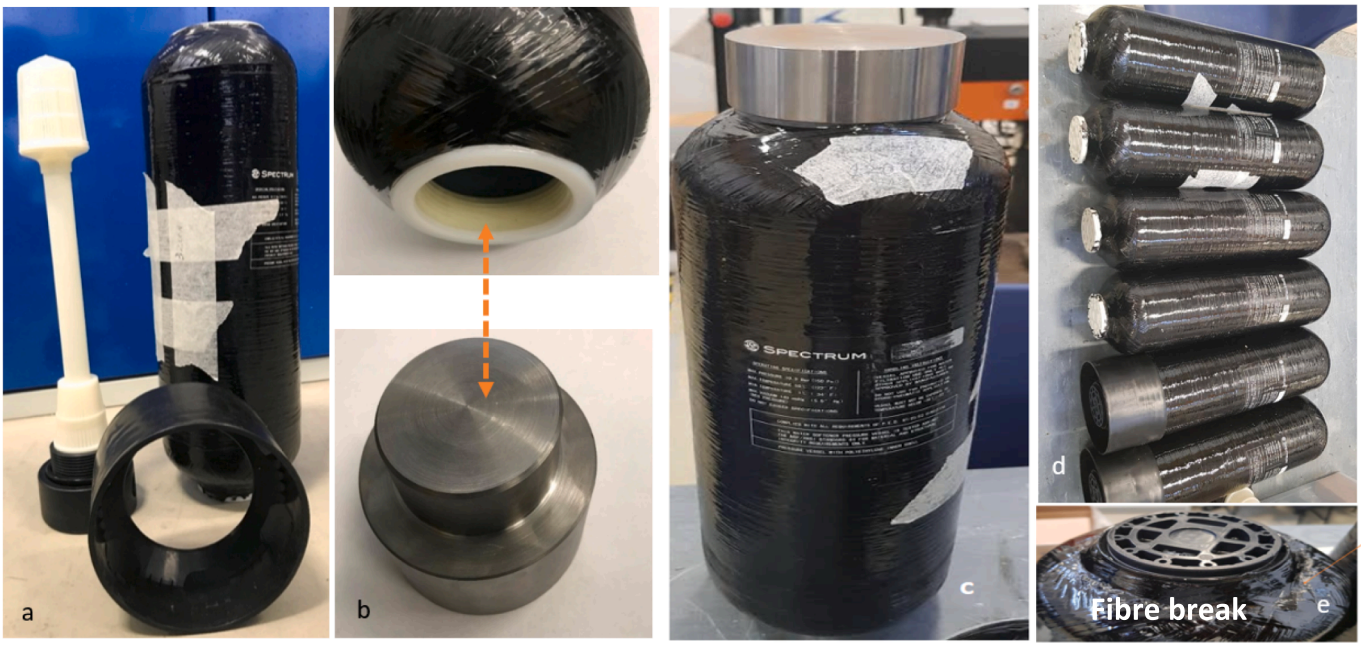


**Fig. 1.** Show (a) the disassembled vessels for the testing (b) vessel and cap for axial test (c) prepared composite vessel for the experiment (d) samples pressure vessels (e) previously indented and compressed vessel.

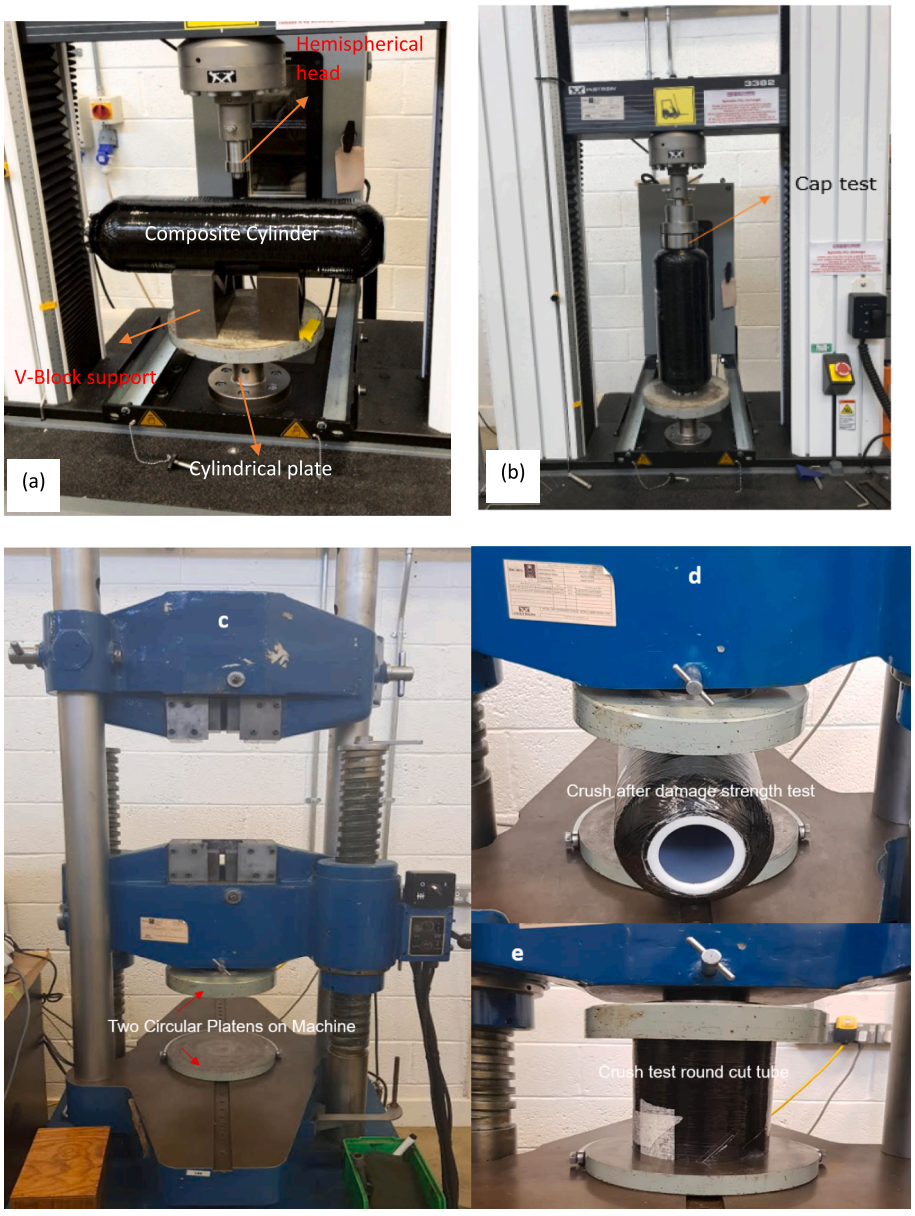


**Fig. 2.** (a) Instron machine with the vessel ready for compression testing in the transverse (b) in the axial direction (c) Intron-XH03 equipment having a 600 kN load capacity (d) vessel in between two circular platens (e) round cut pressure vessel.

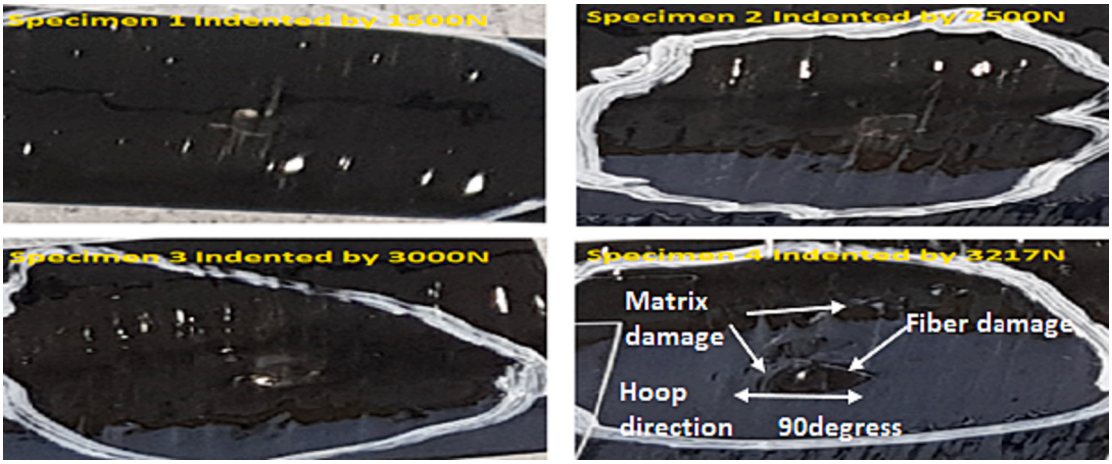


**Fig. 3.** Morphology of Surface Damage Caused during Indentation Test.

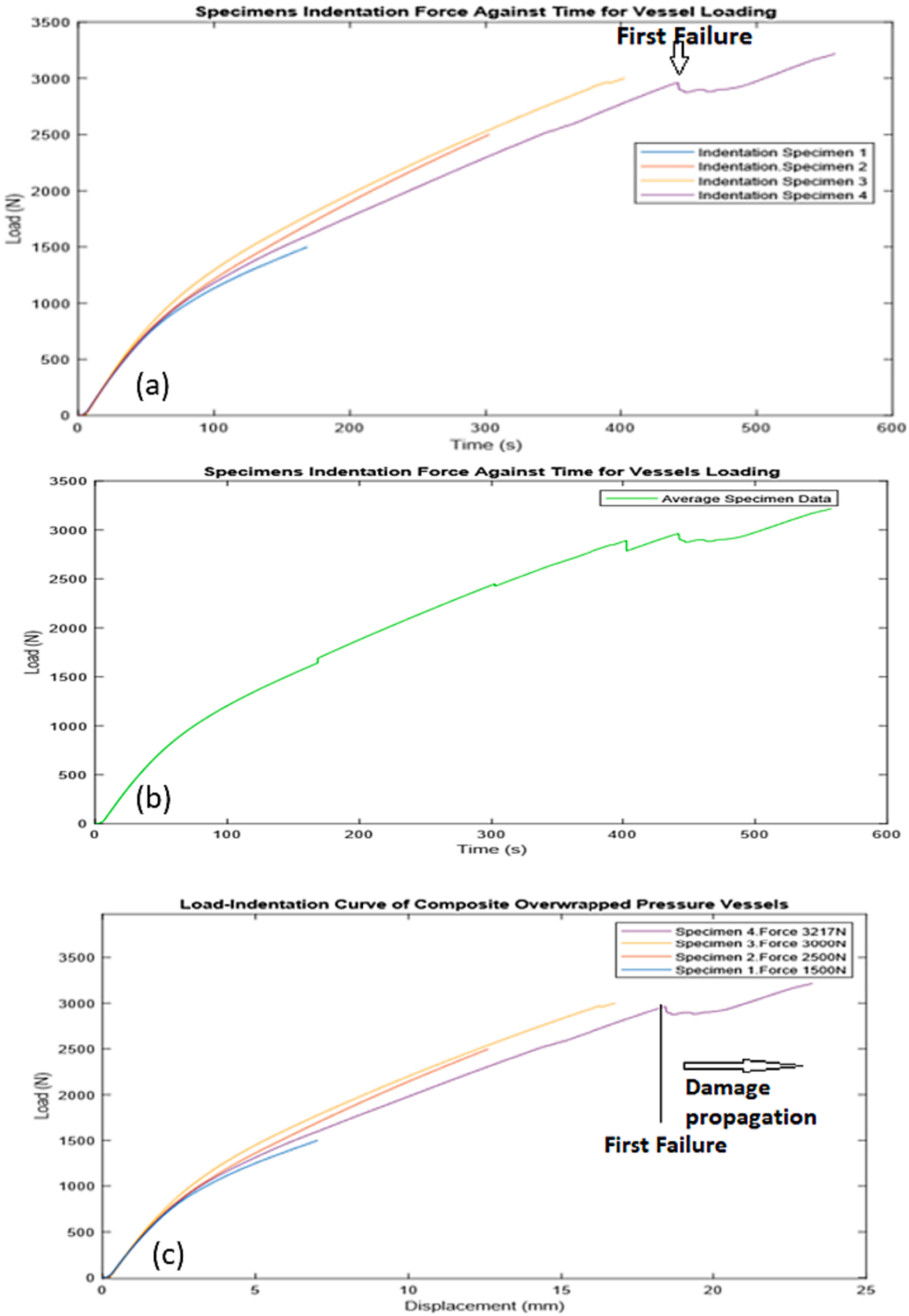


**Fig. 4.** (a) shows load as a function of time of each vessel impacted (b) Mean Indentation Load as a function of Time at a Constant Velocity 2.5 mm/min (c) Indentation Load as a function of Displacement at Constant Velocity 2.5 mm/min.

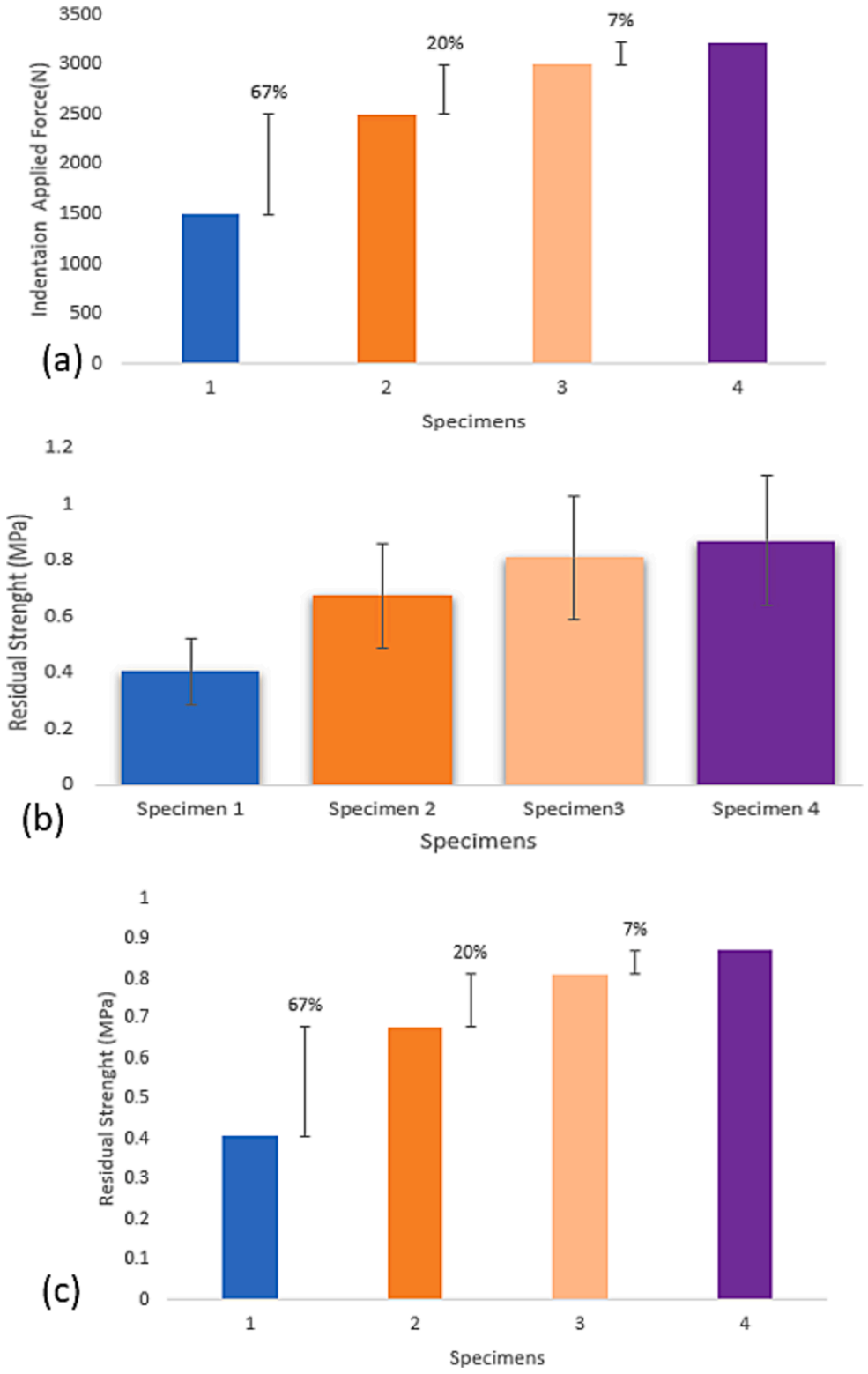


**Fig. 5.** (a) Percentage Change on Each Load on the Specimens (b) Residual Strengths of the Pressure Vessel (c) Residual strength Percentage Change during Impact Test.

study on quasi-static and impact test for damage resistance prediction in composites shells structures present the relationship between impact and quasi-static equivalence on shell structures with instability.

In a different study, Liu and Xu [20] explores the effect of impactor's shape and length at different impact velocity using customised conical and cylindrical ice impactors on steel and CFRP. Results from this study shows that damage of ice impactor is more prominent for sandwich composite specimens, while partial damage is commonly seen in steel specimens. Also, Karakuzu [21], Shyr and Pan, Kobayashi and Kawahara, Mouti et al., Weaver [22–24] examined the impact damage of laminates using strip impactor oriented at different angles, found that the delamination area and residual load capacity decrease as impact

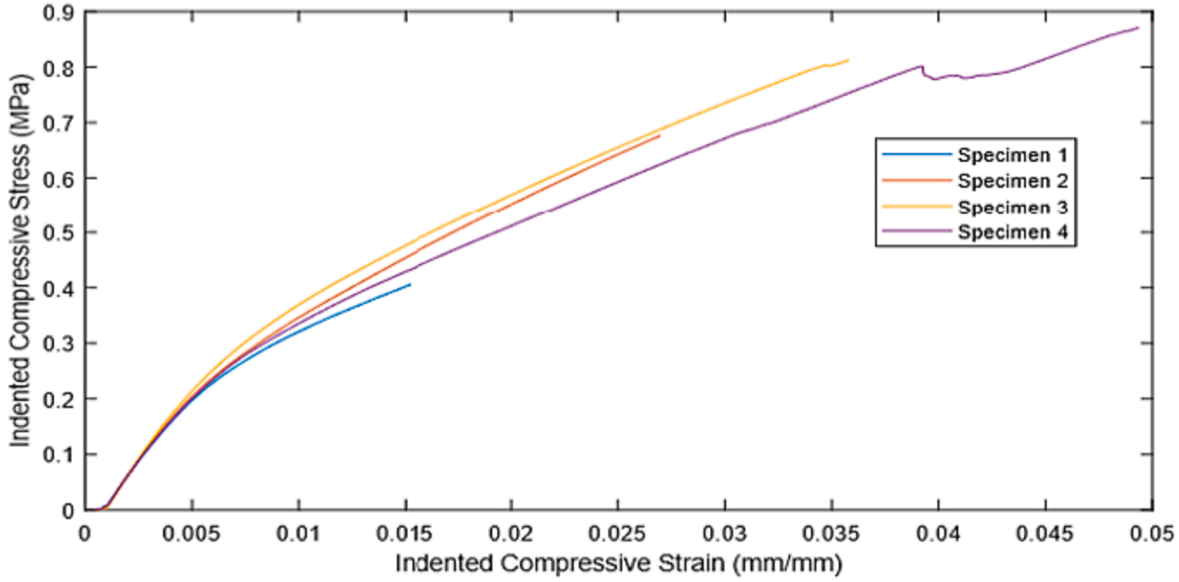


**Fig. 6.** Indentation Stress-Strain Curves for the 4 vessel Specimens.

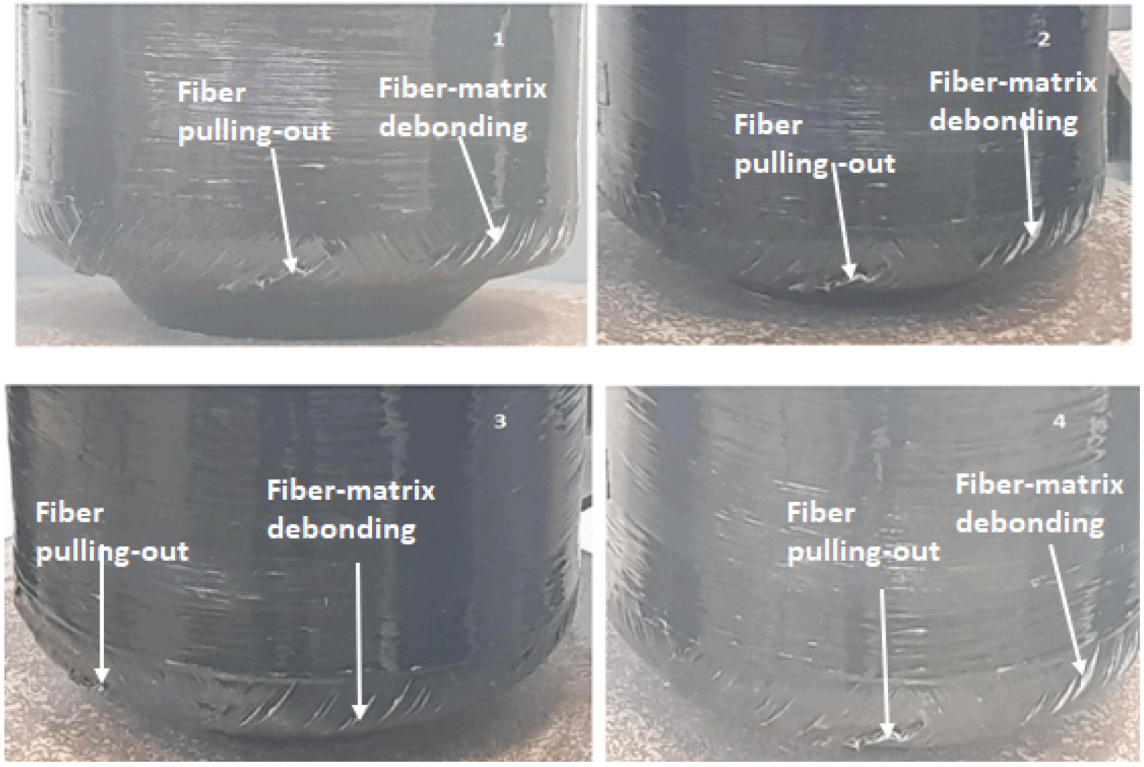


**Fig. 7.** Damage After Compression:(1) Indented at 1500 N, (2) Indented at 2500 N,(3)Indented at 3000 N and 94) Indented at 3217 N.

angle increases. Njuguna et al. [25] and Kim et al. [26] found both the velocity and the diameter of waterjets are crucial factors on carbon fibre reinforce polymer (CFRP) damage extents in a study entitled impact damage of composite laminates with high-speed waterjet. The study of Banik et al. [27] on composites for energy storage containing lithium-ion batteries found that low impact energy events (≤4 J) had negligible effect on the residual energy storage capacity of the lithium-ion battery, although higher energies (≥6 J) caused an internal short circuit due to excessive plastic deformation and crushing.

Other studies in the literature covered low impact energy damages in COPVs and established that damages in the vessels result in performance decrease. This is expected as the induced damage undermines the structural integrity of the vessel as such the reduced performance in terms of strength. Previous work of Tuo et al. [28] studied two methods of indentation and low impact energy and has reported that the indentation of the vessels with the same peak loads as the impact test can be used as a substitute method in studying the damage evaluation. Most of the numerical analysis however has been focused on the composite fracture constitutive model due to lower failure strain of these materials. However, it is also important to evaluate the residual strength of the composite/liner subjected to external impact.

The worldwide climate change crisis, about depletion of the ozone

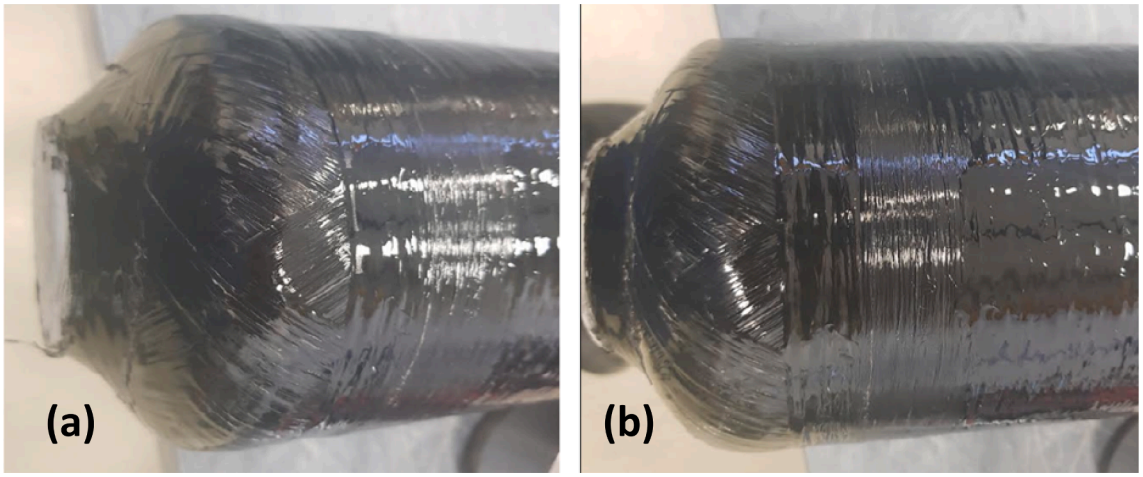


**Fig. 8.** Damage After Compression:(A) without Indentation and (B) Without Indentation.

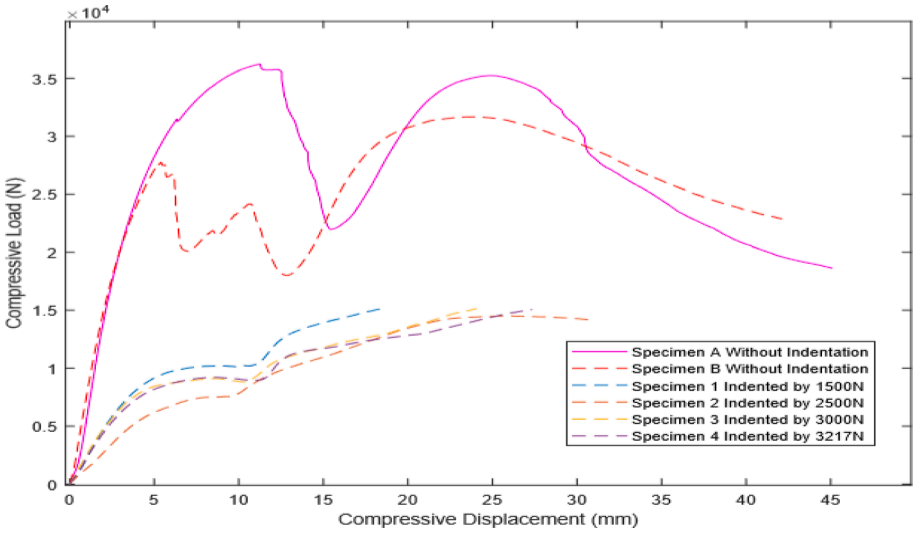


**Fig. 9.** Compared Load-Displacement Response with and Without indentation Specimens.

layer, global warming, air and water pollution due to greenhouse gases emission especially carbon dioxide and methane has brought about global drive toward a carbon neutrality and net zero economy. This resulted in decreased reliance on fossil fuel base energy sources and geometric increase in renewable energy vectors to transit from the fossil base energy sources to renewables Njuguna et al. [25,29]. However, in recent years hydrogen need to be stored in pressure vessels at pressure up to 70 MPa, and minimising both weight and cost of vessels for application in the transportation sector [30,31]. Storing hydrogen is a challenge because it has high energy content by weight, and a low energy content by volumes well noted by Reynolds et al. [31], Nguyen et al. [16] and Maus et al. [17]. Therefore, this makes hydrogen storage a challenge specifically in the automotive applications. Challenging barriers to the widespread adoption and utilisation of hydrogen as energy carrier are the development of reliable, safe, compact and cost-effective technologies for its storage Allen et al. [32], Barral and Barthelemy [33].

The current study investigates the performance of composite overwrapped vessels having thermoplastic liners after impact. The vessels studied in this study is made up of a high-density polyethylene liner and glass fibre overwrapped. Therefore, this research investigated the load bearing capacities of the indented vessels in axial and hoop directions to ascertain the level of impact using experimental approach and NDT on such vessels after damage as well as establish structural performance.

## 2. Materials and methods

### 2.1. The composite pressure vessels (Hydrogen pressure vessels type IV)

The composite pressure vessel analysed in this study is an industrial product produced utilising a thermosetting, orthophthalic unsaturated polyester material matrix, that has been enhanced with a portion weight of 70 % of Tex type E utilising constant glass fibre with lay up of $[(90/40/45)_n]_S$ with even hoop and helical thickness of 8 mm. Details of the vessels used for the physical experiment and history are shown in Table 1. The vessels are all lined internally with a layer of high-density polyethylene (HDPE) produce through a rotational moulding process to give, among other objectives, a barrier against diffusion of gas. The selected properties for the glass fibre and the liner are shown in Table 2.

### 2.2. Samples preparation

The purpose of the tests is to determine vessels structural performance owing to low velocity axial and transverse loading. Hence, the cylinder samples are disassembled as part of the sample preparation for the testing process as illustrated in Fig. 1a. The steel cap provides a rigid

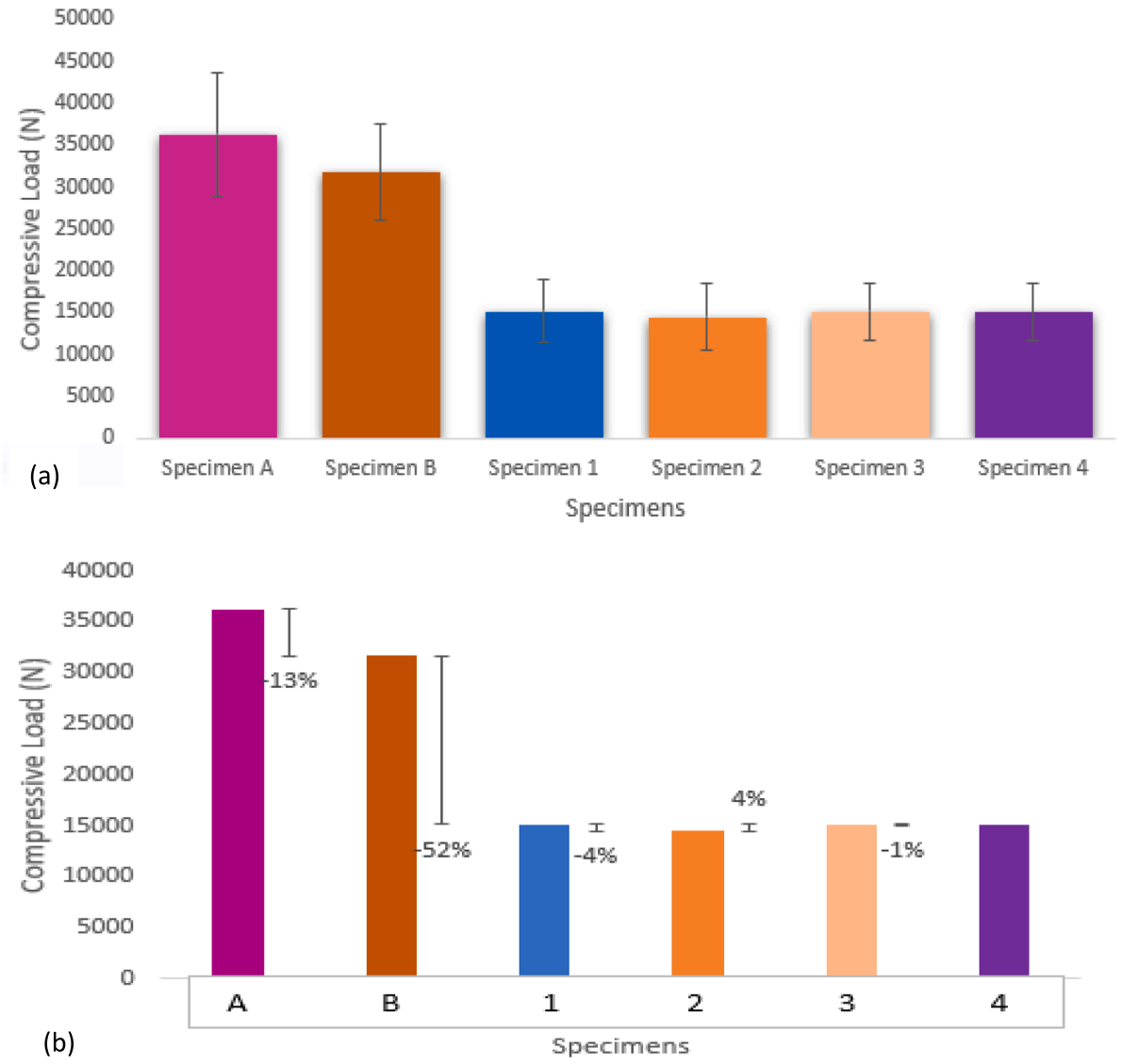


**Fig. 10.** (a) -Compressive Load Applied to the Specimens (b) compressive Load Percentage Change on the Specimens.

support for the vessel in order to withstand the axial force during the experiment see Fig. 1b. For effective experimentation the vessels were dismantled, as illustrated in Fig. 1. The preparation involves meticulous plan for the effective axial and hoop compression. The head of the cylinders are changed with a steel cap during the axial compression on the vessels as shown on Fig. 1b. In addition, the centroid of the vessel is determined and delineated with tape as shown on Fig. 1b to enable efficient compression in the hoop or transverse configuration (see Table 3) for the details of cylinders, tests configuaration and the loading speed. For example, column 1 give the impact condition/scenario of the vessels. While, column 2 shows configuaration of the vessel during tests which could either be axial, transverse direction.

### 2.3. Characterisation

All the composite vessels were visually examined before the test, and steel cap fitted as shown in Fig. 1c. Two of the cylindrical vessels were in a good working condition, no imperfections or damages was determined in the samples, four of the previously indented vessels had signs of fibre fracture at the bottom of the vessels (Fig. 1d). Meanwhile, Fig. 1e shows damaged zone on the bottom of the vessel. All the samples were approved for the testing phase accordingly. Furthermore, an additional evaluation is needed to assess the damage after test.

Microscopy study was conducted using microscopy options capability of the Mitutoyo HM-200® Series Micro Vickers Hardness Testers that is equipped with an included USB color mega-pixel vision system supported by AVPAK® software for automatic indentation measurement.

Dolphitech uses a unique 2D matrix array architecture to produce a transducer module (TRM) with 16,384 elements and an active aperture of 32 × 32 mm. This is achieved using 128 transmitting electrodes which are positioned across 128 receiving electrodes, with each crossing point forming an individual element with a pitch of 0.25 mm. This provides unparalleled data capture and resolution, which, when combined with frequency range from 1.5 MHz to 10 MHz, which gives the ability to inspect a wide range of materials. However, the pipe was scanned using the 1.5 MHz transducer (low frequency, TRM-EA-1.5 MHZ) as it provides higher penetration through the COPVs test samples. The gain was set at 6.5 dB and the velocity 2777.78 m/s. After the data is acquired, a post-processing was accomplished using probe and basic shapes such as circle, lines, and rectangles to further delineates zones of interest. This post-processing tools enable the measurement of length, diameter, perimeter, area, circumference and depth of defects or delamination in the units of mm as per our study requirement.

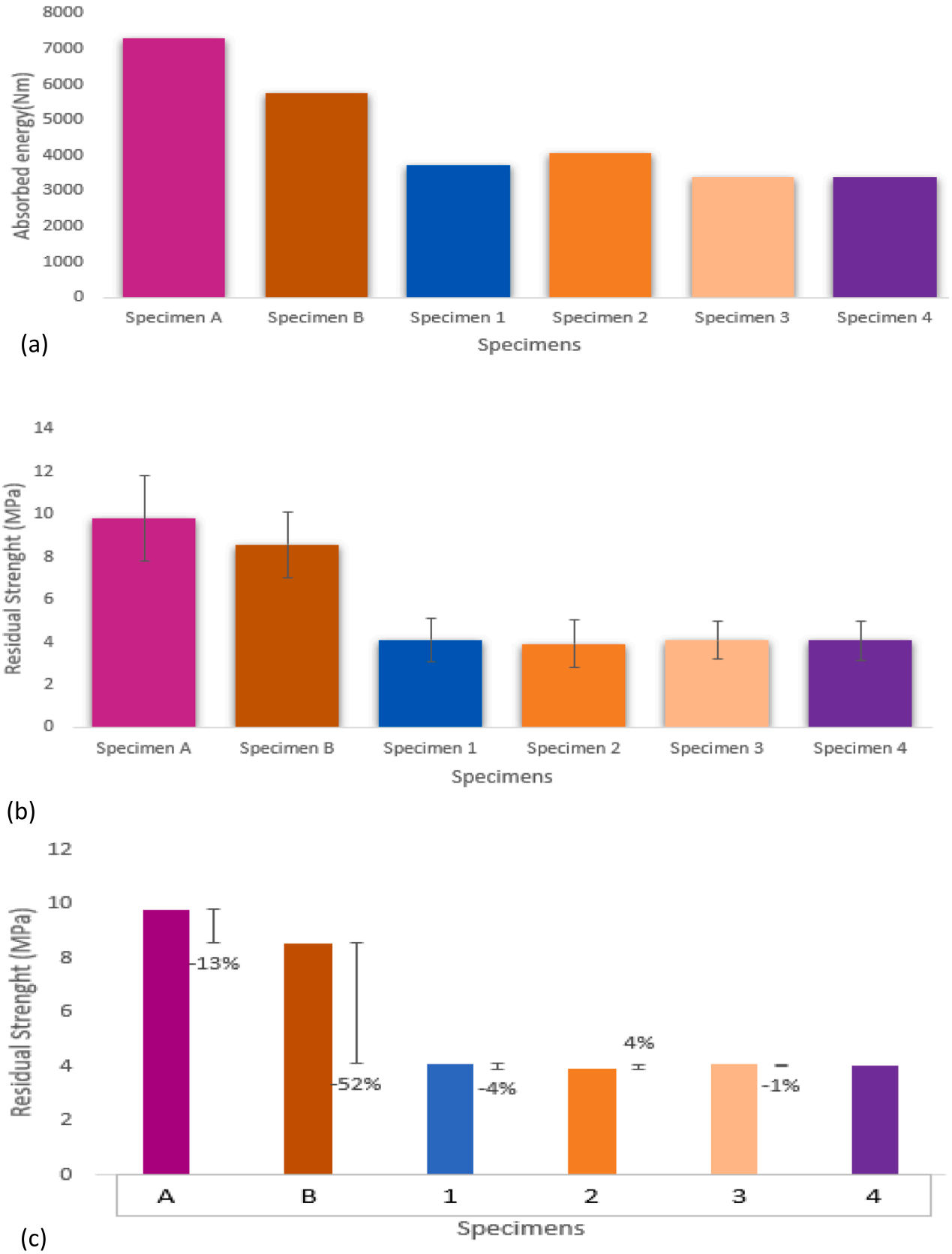


**Fig. 11.** (a) Absorbed Energies of the Specimens from Compression Test (b) Residual Strength of the Specimens after Axial Compression (c) Residual Strength Percentage Change After Compression.

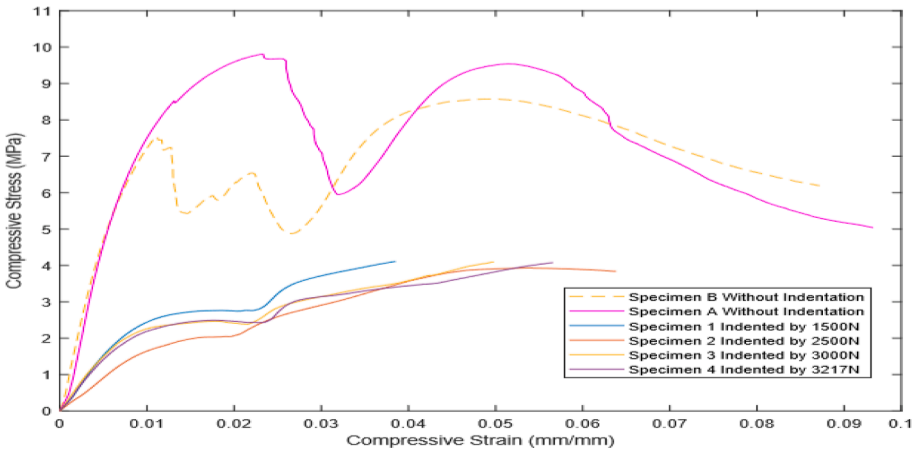


**Fig. 12.** Compressive Stress–strain Response of with and without Indentation Specimens.

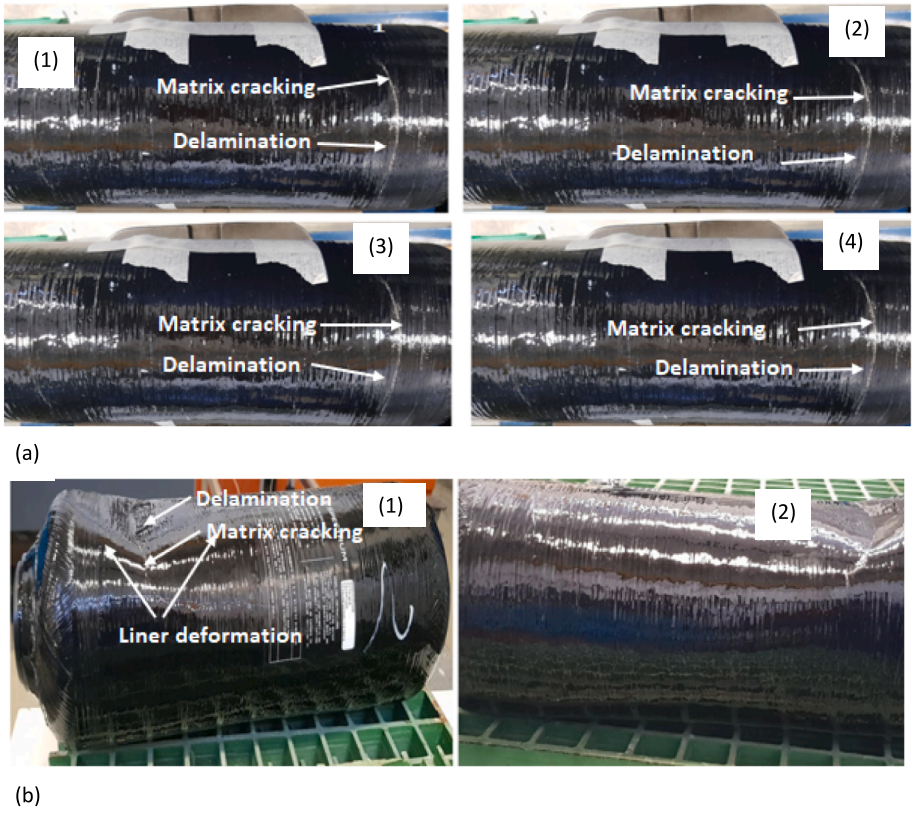


**Fig. 13.** (a)-Damage After Crush Test:(1) Indented by1500N, (2) Indented by 2500 N, (3) Indented by 3000 N and (4) Indented by 3217 N (b) Damage After Crush test:(1) without Indentation (2) without Indentation.

### *2.4. Testing*

#### *2.4.1. Indentations/dent damage - set up, loading conditions*

A quasi-static indentation examination was selected based on ASTM D6264 standard. Quasi-static indentation represents a functional analogue for mechanistic assessment of low-velocity impact damage (47).

The test is performed with Instron Universal testing machine 3382 model of 100 kN capacity. The load was applied at a constant speed of 2.5 mm/min, to the cylinder both non– compressed and compressed cylinders were tested until failure. Five samples were tested in each case and the average used to evaluate the compression strength of the composite pressure vessels studied under this test category.

The quasi-static compression test was performed at speed of 500 mm/min. The tests was also executed using an Instron 3382 machine at room temperature 23 °C. The universal test machine was equipped with a high-speed data acquisition system of load–displacement and stress–-strain. A hemispherical head with a diameter of 15 mm made from steel was selected as the indenter as shown on Fig. 2(a). From the size of the indenter, it can be related to flying debris or rock/stones that the hydrogen pressure vessel can get in contact with during the transportation, storage and in the roadway. This was connected in the load cell of the machine to facilitate the impact tests.

The experiment was performed with no pressure in the vessels (internal pressure = 0). Using the Instron machine Bluehill software and application loads settings of 1500 N, 2500 N, 3000 N and 3217 N were

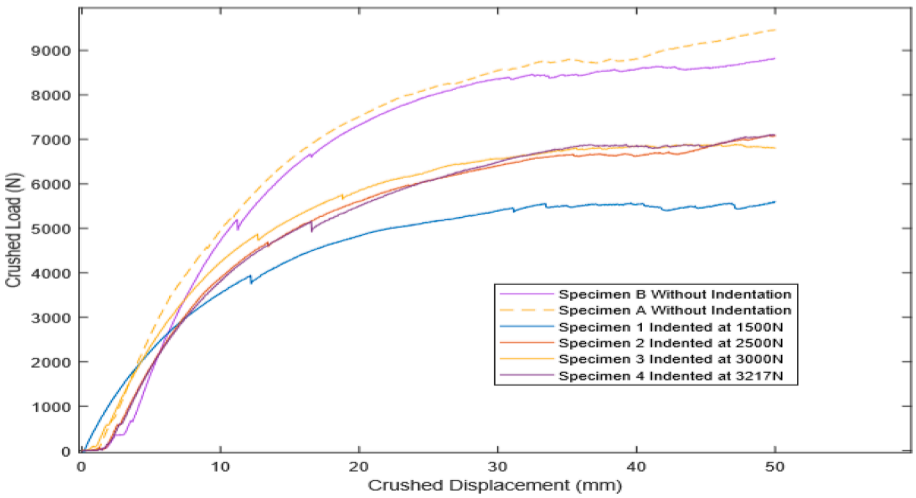


**Fig. 14.** Compared Crush Load-Displacement Response for with and Without Indentation Specimens.

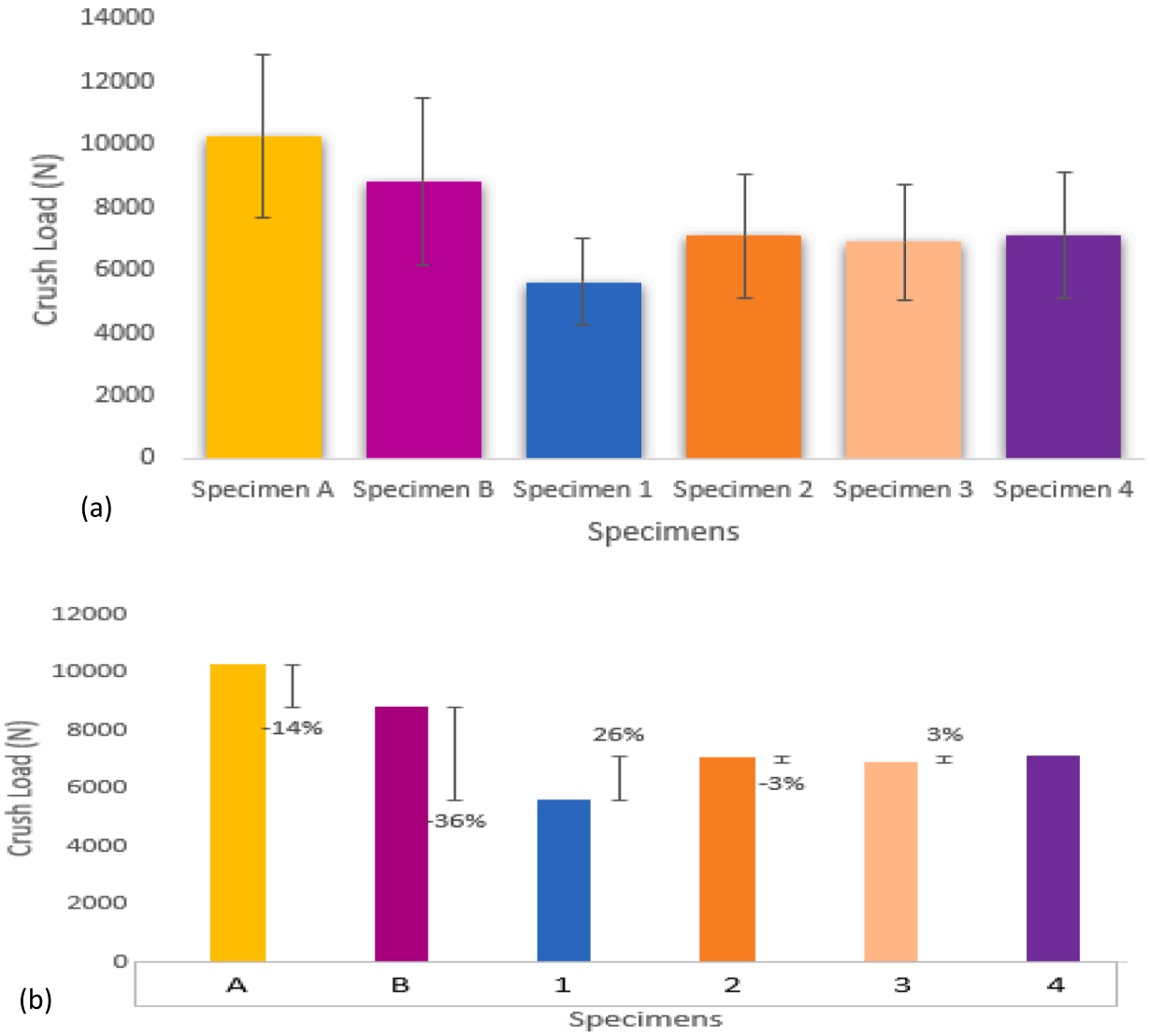


**Fig. 15.** (a) Crush Load applied to the Specimens (b) Crush Load Percentage Change on the Specimens.

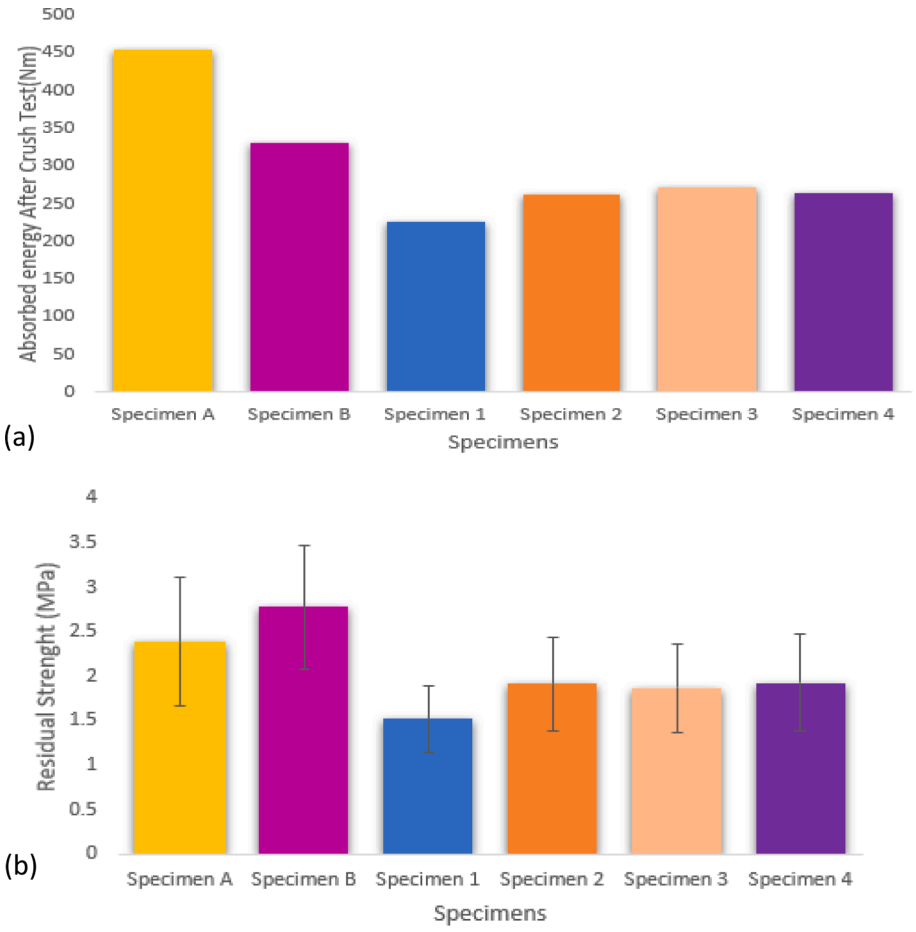


**Fig. 16.** (a) Absorbed Energies of the Specimens from Crush Test (b) Residual strength of Specimens After Crush Test.

used in various cylindrical vessels. The loading selected are typical represetnation of endurance levels of 300 kg anchor drop damage in storage and transport conditions where the cylinders in a stack racking or objects in offshore transport and static point load endurance in case of hydrogen COPVs for offshore hydrogen storage. The equipment was set up to stop after reaching the needed load (the applied load was the control specification), the load was applied at a continuous rate of 2.5 mm/min. All the samples were indented at the centre utilising the same head geometry attached to the load cell of the Instron machine as seen in Fig. 2(a).

### 2.4.2. *Compression-after-damage strength test*

A steel cap was connected to the head of the pressure vessel, so it can support the compression force, see Fig. 2b. The axial compression test is conducted to examine the compressive strength of the hydrogen pressure vessel. The examination was performed with the universal testing machine equipment with a capability of 100 kN. The load was applied at a consistent speed of 2.5 mm/min to the pressure vessel both the indented and without indentation vessels were examined until failure.

### 2.4.3. *Crush after-damage strength test*

The tests were performed using a universal testing machine having a 600 kN capability hydraulic loading Fig. 2c. The sample was placed in between two circular platens (shown on Fig. 2d). The platens maintained parallel to each other before the initiation of the test and also maintained to the end of the examination (Fig. 2d). The load was applied at a consistent speed of 2.5 mm/min to the hoop region of the vessel both the indented and without indentation vessels were analysed until failure. Lastly an axial crush examination was done on the round cut vessels (Fig. 2e). The automated data acquisition system of Blue Hill (Instron-XH03) was utilized to get the load–displacement curve of the crush examinations. During the tests, the load–displacement data was recorded as a function of time at intervals of one second.

The experimental testing on composite vessels, the testing techniques include quasi-static compression in the transverse direction and axial compression-after-damage testing.

The Instron device can be utilised for quasi-static indentation by applying a load at a desired speed based on either test standard or specific requirement. The samples were again visually inspected before the test and only samples with no visual damage were taken to testing. Test samples are then mounted in the test rig for compression tests as demonstrated on Fig. 2. A hemispherical head with a diameter of 15 mm made of steel as shown in Fig. 2b was used for the test in the transverse direction. The test simulates damage on the typical point load on the composite pressure vessels during its use, transportation, storage and in the event of other potential impact [33]. The compressed gas composites pressure vessels were mounted and supported by two V-block fixtures of 90° angle made of steel standing on a circular plate, as presented in Fig. 2a to damage the pressure vessel. The Instron machine was set up to cause a static compression by applying loads of 1200 N, 2200 N, 3200 N and 4200 N at a constant speed of 500 mm/min as shown on Fig. 2 under different test configurations.

Next, the indentation (puncture) compression tests were conducted according to ASTM D6264 to determine the damage resistance of the hydrogen pressure vessels subjected to a concentrated indentation force in a set up shown in Fig. 2 (a, b and d and e).

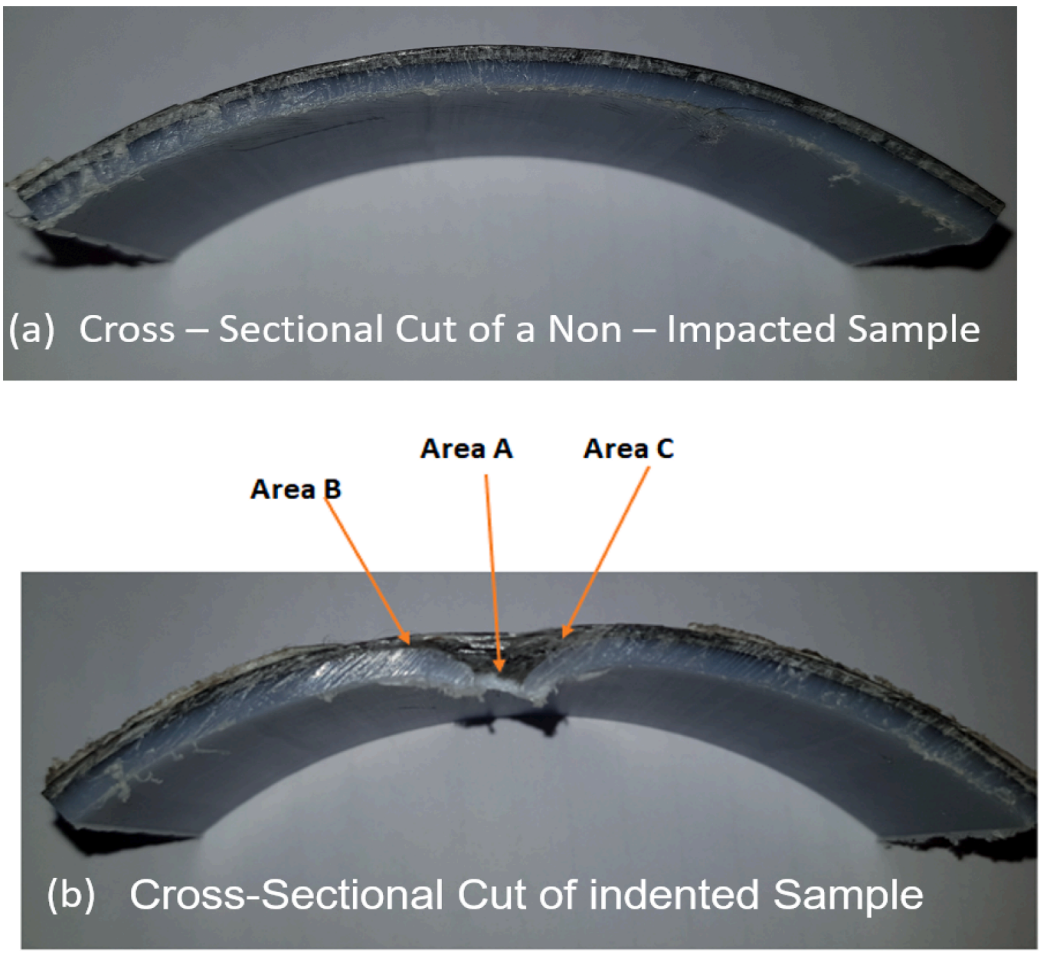


**Fig. 17.** (a) Cross- Sectional Cut of the Indented Area (b) Cross-Sectional Cut of indented Sample.

## 3. Results

### 3.1. Damage characterisation results

Fig. 3 shows the morphology of surface damages caused by quasi-static indentation. In specimen 1 (1500 N) and specimen 2 (2500 N), the impact damages were not significant around the area of indentation yet there were splitting around the local area in the fibre direction. In specimen 3 (3000 N), the splitting around the impact point propagates in the fibre direction and finally, for specimen 4 (3217 N) there were considerable splitting and also matrix damage around the impact point.

#### 3.1.1. Graphic Results: comparison of the load as a function of time

Fig. 4a shows load as a function of time of each vessel impacted. At 1500 N (Specimen 1) as well as 2500 N (Specimen 2) impact, it can be seen that the wall of the vessels deflects between 0 and 300 s. This confirms that the vessels can support both loadings for a longer time period, without any deformation or splits. At 3000 N (Specimen 3) impact, it can be seen that the wall surface of the vessel still deflects in between 0 and 400 s, Nonetheless, as loading increases at 3217 N (Specimen 4) impact, the vessel elastic limit is reached at 450 s and afterward, the first failure initiation begins. Before the first failure, the load rapidly raised as the deflection increased. Nevertheless, after the first failure, the load rise was significantly reduced as the deflection increases in between 450 and 560 s, and also significant vibrations loads were observed. The first damages critically reduced the stiffness of the composite vessel and the damage slowly propagate as much as the time of the maximum deflection. As the impact load increase, the response time also rise. Fig. 4b shows the average indentation force against time for the pressure vessels. As it can be seen a similar trend is obtained when compared to Fig. 4a.

#### 3.1.2. Comparison of the load as a function of displacement

Results of the 4 specimens shows the responses of each vessel under specific loading condition (Fig. 5). Generally, all loading regimes demonstrate a comparable force–displacement response. An initial elastic phase was observed to approximately 16 mm displacement where upon a slope change occurred, and a secondary regime of lower gradient continued to as much as 23 mm displacement as shown on Fig. 4c. During this second phase also known as the damage propagation phase, some stiffening of the structure (vessel) with raised load–displacement was observed.

Fig. 5a shows the change in percentage of every force applied on each specimen and it can be seen that the least amount of percentage change is between specimen 3 and 4 is 7 %. On the other hand Fig. 5b reveals the residual burst strength of the composite vessels. In all specimens, residual burst strength raised with raising the impact force/indentation force. Since all the specimens are made of the same material, for this reason, the modulus is the same, and the indenter or impactor utilised during the experimentation had a constant size of 15 mm. Therefore, the burst strength is proportional to impact force. The residual percentage change is proportional shown on Fig. 5c. Similar values are obtained for as in Fig. 5a.

#### 3.1.3. Comparison of the compressive stress as a function of strain

Specimen 1 and 2 shows the elastic region of the graph, the material is under uniform stress and strain. This is presented on Fig. 6 blue and Orange lines as shown. The slope of graph represents the Young's

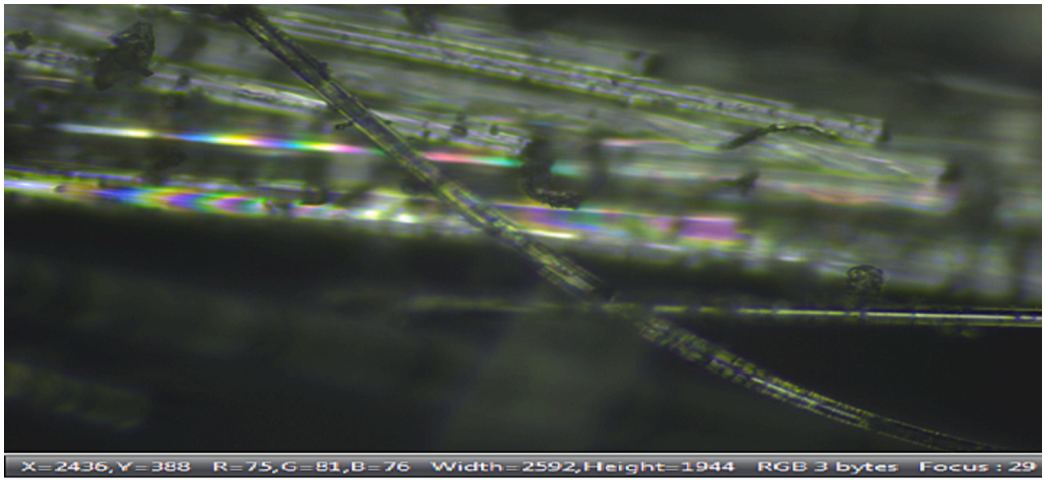


(a) Microscopic View of Area A reveals Fibre Cracking

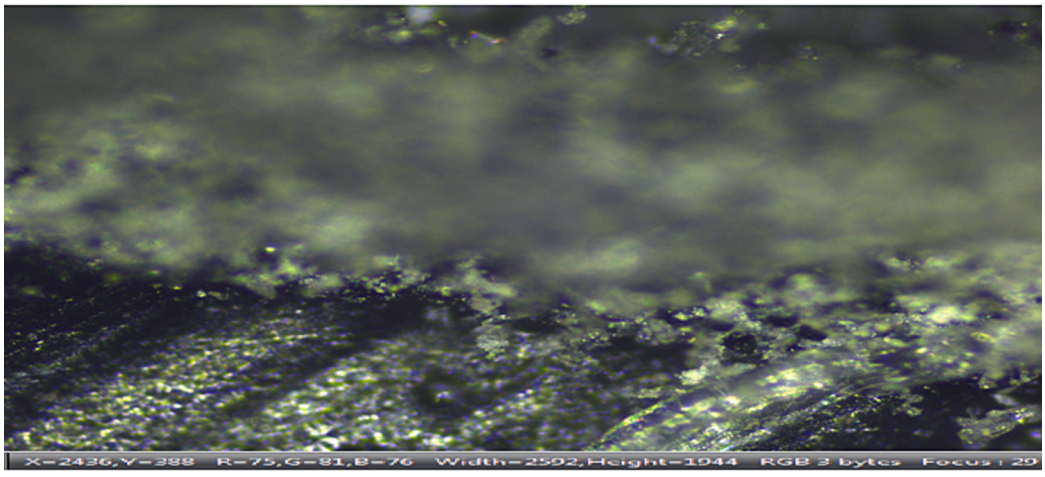


(b) Microscopic View of Area B reveals Debonding

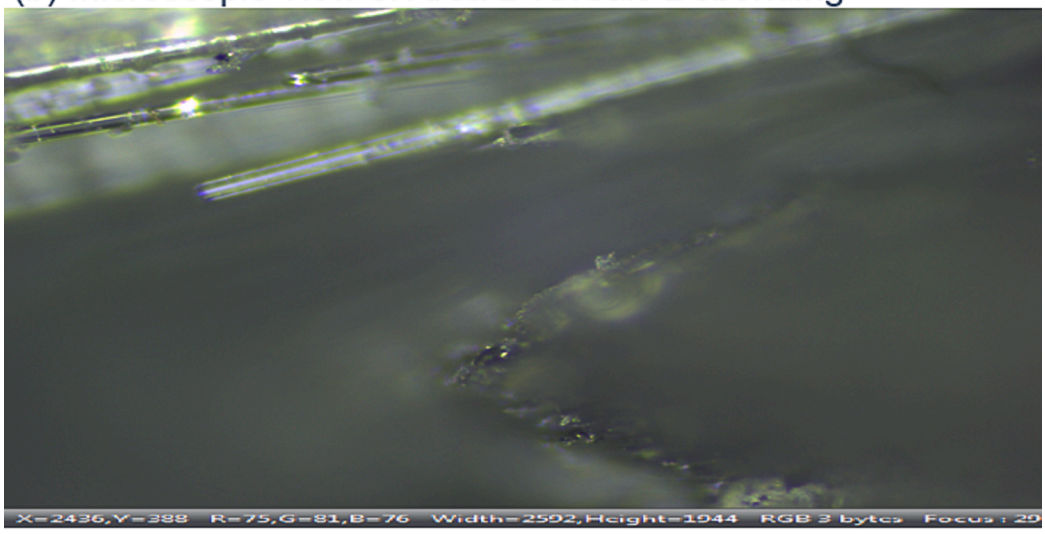


(c) Microscopic View of Area C reveals Fibre Breakage

**Fig. 18.** Microscopy results (a) fibre cracking (b) debonding (c) fibre breakage.

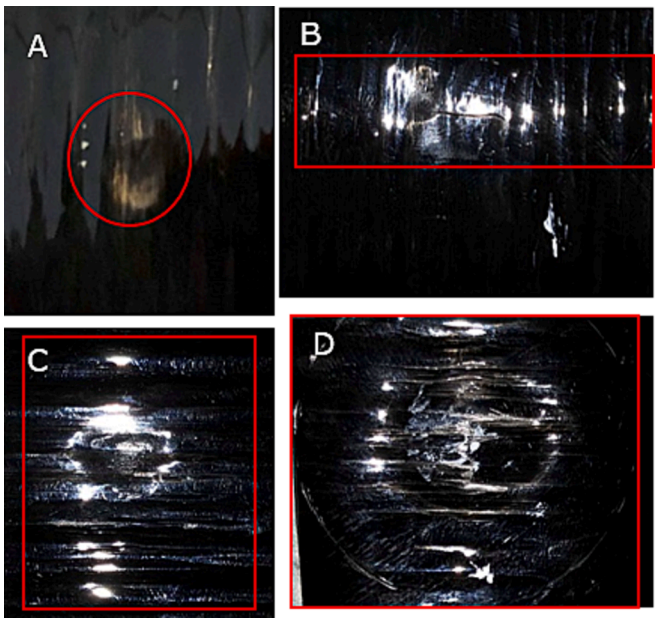


**Fig. 19.** Visual inspection: (a) Pressure vessel under Load of 1200 N (b) Pressure vessel under Load of 2200 N (C) Pressure vessel under load of 3200 N (D) Pressure vessel under load of 4200 N.

modulus. Specimen 3 has reached the yield point loading at strain 0.035 and Specimen 4 has exceeded specimen hardening region, the material ultimate strength has been exceeded resulting in the first failure before entering the second region behavior (see Fig. 6) the purple for more details on the material behaviour under test.

#### 3.1.4. Compression-after-damage strength test results visual inspection

Fig. 7 shows all the visual failure on the impacted specimens. In all cases, failure occurred in the bottom support region of the vessels. The outer layer fibres peel off began in the region where fibre damage had actually previously been brought upon in this case, not the impacted location. This was because the impacted vessels had defect such as fibre fractures as seen in Fig. 7. The reason for the external layer of the fibres peel off was that the fibres experienced high shear stress due to compression. In addition, those regions have experienced micro-buckling under huge stress. This causes huge shear stress throughout the external laminae at the boundaries between the damaged and undamaged fibres, which in turn creates the damaged fibres to debond as well as peel away from the vessel. Ultimately, as internal pressure increased, rupture occurred in the peeled area. Since fibres are the major load-bearing component in the pressure vessel, the decrease in burst pressure is mainly identified by the extent of fibre damage.

As seen in Fig. 8 the vessels without impact showed no considerable visual damages since the vessel had actually no inflicted area on the fibres, for this reason, could endure a higher pressure/ load before failure is reached.

### 3.2. Comparison of the load as a function of displacement

Fig. 9 shows the load–displacement responses of thehHigh-density polyethylene liner at 23 °C. The impacted specimens in all cases before the first failure, the measured load increased almost linearly with some vibration as the displacement increased; however, the slope of the load increase significantly decreased after the first failure between 5 mm and 10 mm this was as a result of the outer layer fibres peel off where fibre damage had previously been inflicted not the impacted location. This was because the impacted vessels had defects such as fibre fractures as seen in Fig. 1e. Looking at the Fig. 9 showed a secondary regime of lower gradient continued to as much as 25 mm displacement. This was validated in Kim et al [26] study in that during this second phase also known as the damage propagation phase, some stiffening of the structure (vessel) with raised load–displacement was observed. Also, similar behaviour was also observed in the load- displacement response of the undamaged vessels but with a steeper slope at the early stages. Fig. 9 clearly shows that the first failure for undamaged vessels occurred at a higher compressive load and lesser displacement compared to the damage vessels proving that fibres are the major load-bearing component in the pressure vessel, the decrease in loading capacity is mainly identified by the extent of fibre damage. A notable observation drawn from Fig. 9 is the divergent nature of the graphs this can be justified to two condition one positioning of the specimen in the machine during each test and the imperfection of the impacted specimen as a result of previous impact and compression on the specimens.

#### 3.2.1. Compressive load after test

Fig. 10 (a) shows that the compressive load is directly proportional to the compression applied to the specimens and the undamaged specimens tend to have a higher compressive load capacity compared to the impacted vessels. This was expected as the pressure vessels have similar physical and mechanical properties. The fibres are the major load-bearing component in the pressure vessel, the decrease in loading capacity is mainly identified by the extent of fibre damage (33). Fig. 10b reveals a significant drop of 52 % in loading capacity of all the impacted vessels. This is high as a result of two condition firstly the impacted vessels used had some imperfect from previous damage (Fig. 2e) and secondly as a result of the current impact test.

#### 3.2.2. Energy absorbed during compression

Fig. 11 (a) shows that the higher the compression loading, the higher energy a material dissipates. Most compression energies were dissipated by the plastic deformation of the high density polyethylene (HDPE) liners [5,6,25]. Since the undamaged vessels had no fibre damage they tend to withstand a higher compressive load hence higher energy was absorbed.

The residual burst pressure critically depends on the amount of fibre damage in the hoop layers the more the fibre damages the less the residual burst pressure the vessel can withstand. This can be clearly seen in Fig. 11b with the undamaged vessels having a high residual burst pressure compared to the damaged vessels. Specimen 3 showed a slight reduction in compressive strength compared to other damage vessels indicating that the damage is more on specimen 3 as shown on Fig. 11b.

The percentage change of residual strength on Specimens after compression was computed and plotted on Fig. 11c which reveals that the percentage change of the compressive load is equal to the percentage change of the residual burst strength. This shows that the vessels could withstand the load applied without permanent deformation. Specimen 1 appears to have a lower residual strength indicating a higher level of damage present.

#### 3.2.3. Comparison of the compressive stress as a function of strain

The stress–strain responses of all the vessels has similar characteristics as shown on Fig. 12. First, the yield point for all was reached. For both damaged and undamaged vessels, beyond the yield point, specimen hardening commences. Then the specimens first failure and damage propagation starts. However, the corresponding strain at failure decreases for the undamaged vessels at a higher compressive stress and the corresponding strain increases for the damage vessel at a lower compressive stress.

### 3.3. Crushed experiment results: visual inspection

Fig. 13a and 13b shows the damage after crush test of the impact and non– impact vessels clearly the two main damage mechanisms under the compression platen is delamination with some matrix cracking that joins the different delamination interfaces also for the non -impacted vessels

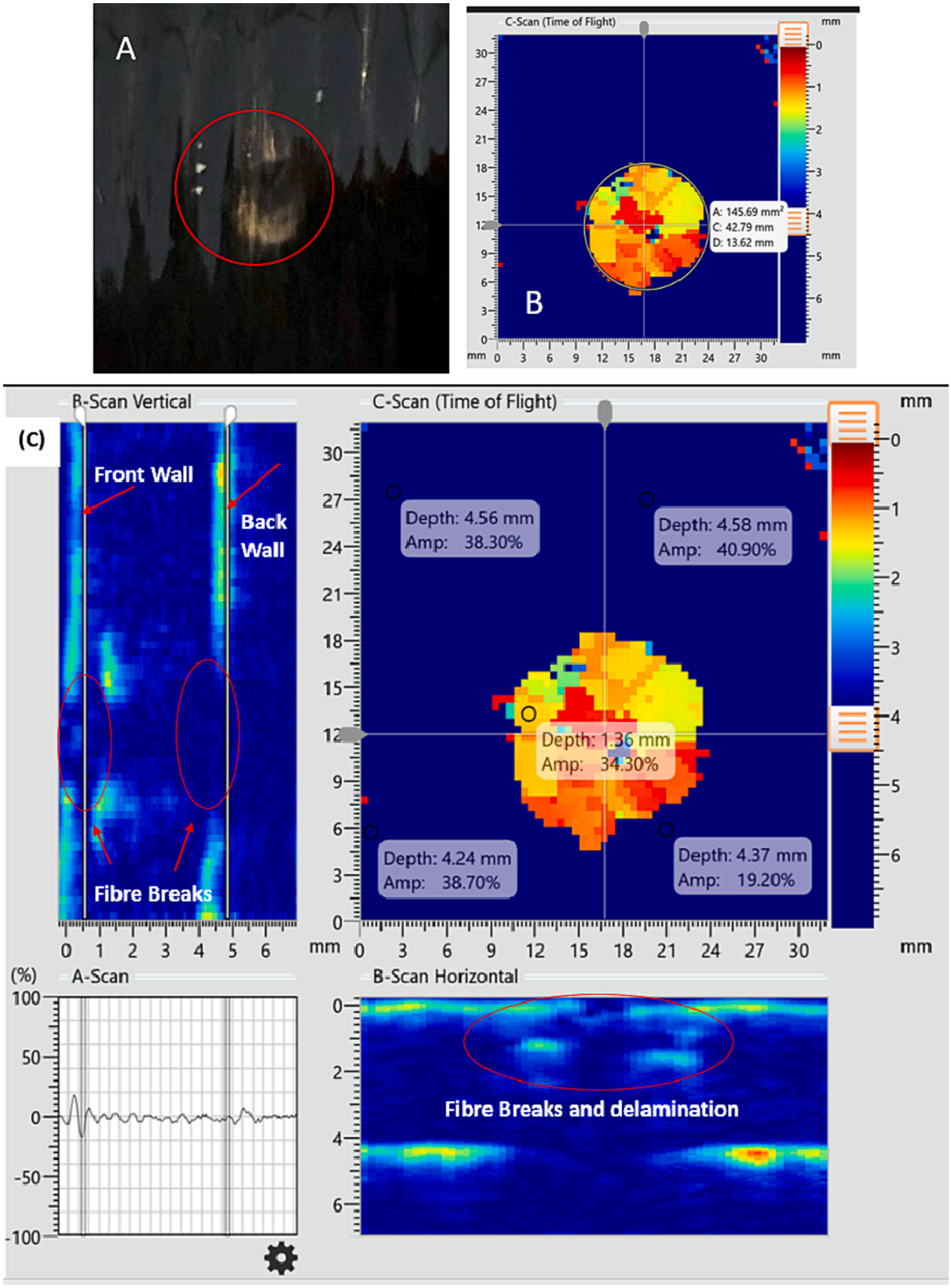


**Fig. 20.** Non– destructive test (a) sample showing the damage region in red (b) C-Scan time of flight (c) shows A, B and C scans with front and back wall, fibre breaks and depths with their corresponding amplitudes.

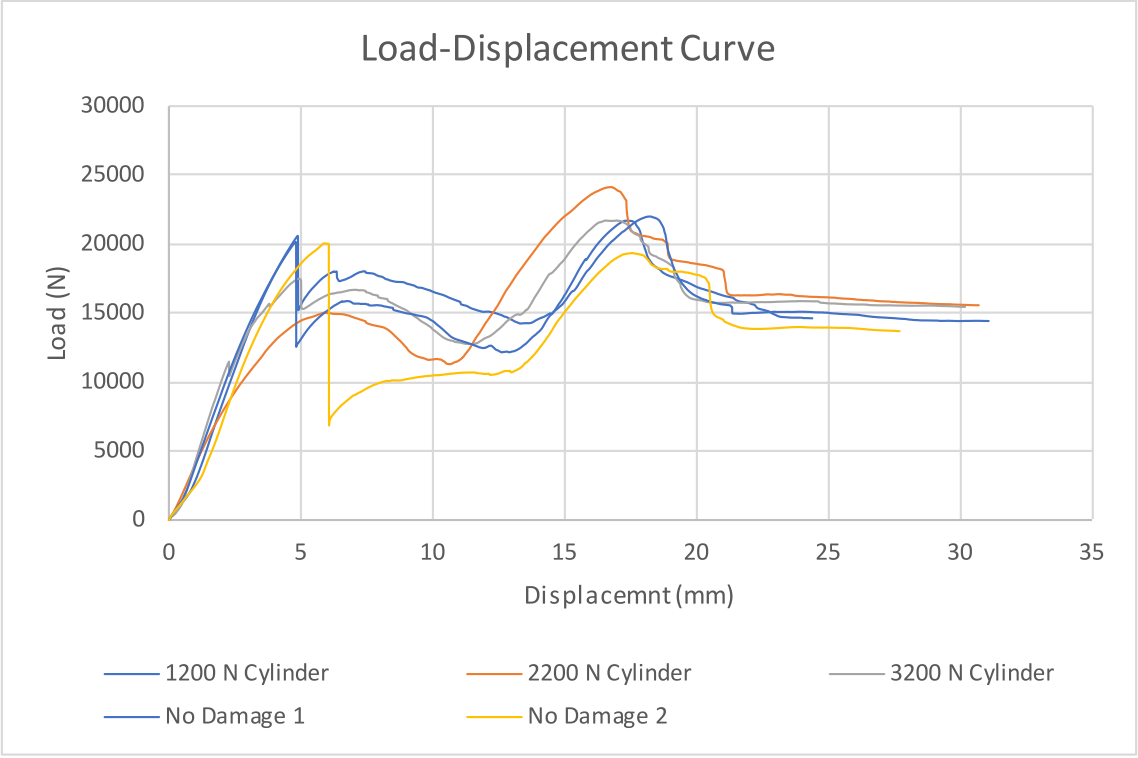


**Fig. 21.** Load- Displacement curve for three cylinders damaged at loads of 1200 N, 2200 N and 3200 N, and two cylinders that have not been damaged before the axial compression test.

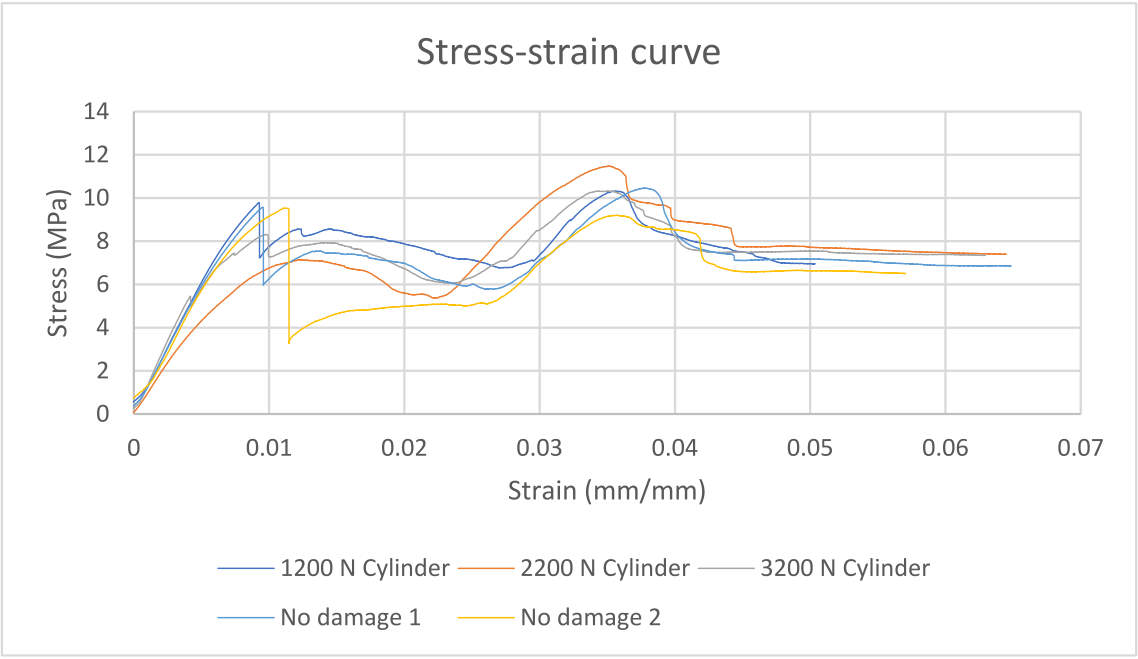


**Fig. 22.** Stress–strain curve for the three cylinders damaged at loads of 1200 N, 2200 N and 3200 N and two cylinders without damage before the axial compression test.

there was deformation of the liners.

### 3.3.1. *Comparison of the crush load as a function of displacement*

Fig. 14 shows the crush load–displacement response of impacted and non-impacted vessels. For one of the non-impacted specimens (Specimen B), an initial elastic phase was observed up to 10 mm displacement at which point a slope change occurred and a secondary regime of lower gradient continued up to 18 mm displacement this was like the impact specimens. For specimen A (non-impacted) the elastic phase was extended up to 39 mm before a slope change occurred and a secondary regime started. This could be as a result of specimen positioning in the machine. This behavior was analysed in Kim et al. [26] reserach work.

The reason for the change of slope is as a result of the first failure which is identified as matrix cracks and delamination.

#### 3.3.2. Crush load after test

The presence of impact damage does influence the load bearing of the pressure vessel as shown in Fig. 15. A reduced value of the peak load can be noticed as compared to the non-impacted specimens. Also, the impact position has a significant result on the initiation of damages (the peak load), whereas its impact on the damages propagation is insignificant. Specimen 1 shows a reduced peak load compared to other impacted vessels indicating that it has damages in the crushed location.

Fig. 15b reveals that specimen 1 has more damage in hoop layer region as a result of its higher percentage change decrease of 36 % compared to non-impacted vessel specimen B and a 26 % decrease compared to another impacted vessel (specimen 2).

#### 3.3.3. Energy absorbed during crush test

Fig. 16a shows that the higher the crush load, the higher energy the vessel dissipates. Most compression energies were dissipated by the plastic deformation of the high-density polyethylene (HDPE) liners. Based on this relationship of crushed load and energy absorbed it can clearly be stated that an impacted vessel absorbs less energy than a non-impacted vessel.

The residual burst pressure critically depends on the amount of fibre damage in the hoop layers. The more the fibre damages the less the residual burst pressure the vessel can take. This can clearly be seen in Fig. 16b. Specimen A residual strength is less compared to specimen B because during axial compression test there were fibre damage to the hoop layer as a result of buckling. Specimen 1 also has a lesser residual strength compared to other impacted vessels. This proves that specimen 1 has multiple damages on it hoop layers not seen with the naked eye.

## 4. Microscopic results

After the tests, a cross-sectional cut of one sample at the indented location with a force of 3217 N (Fig. 17b), and additional sample without indentation (Fig. 17a), were studied by using non-destructive Micro Vickers hardness testing machine HM-200 Series. Microscopy inspection revealed details of the damage caused by a hemispherical head Indenter. There are three notable damage sustained by pressure vessels during impact, firstly fibre damage develops within the contact region (Fig. 17b). The fibre cracking is shown on Fig. 18a develop in the second layer in addition to that of the outer layer. In addition, Fig. 18b reveals fibre debonding and lastly the overall length of fibre crack expand leading to fibre breakage (Fig. 18c).

### 4.1. Quasi-static compression strength during puncture test

Another sets of 4 vessels specimen were further tested to ascertain the level of damage by compression. The initial inspection of damage induced on the vessels at the centre of the vessels at different compressive loads of 1200 N, 2200 N, 3200 N and 4200 N, are illustrated in Fig. 19 (a – d). Based on visual inspection the damage regions are outlined in red as shown on Fig. 19. It is obvious that an increase in the load leads to increase in the damage region as shown.

For a more accurate damage characterisation on the sample, a cross – section surrounding the puncture region in sample ‘A’ was further investigated using Dolphicam2 non -destructive test (NDT) kit.

As it can be seen on Fig. 20(B) the damage characterisation has an area of 145.69 $mm^2$ with a circumference of 42.79 mm for the damaged region. The overwrapped sample ‘A’ is 5 mm thick, relatively flat and the least damage, hence is selected and prepared for an NDT examination. Sample B, C, D are grossly damaged with highly uneven surfaces that will lead to unrealistic results and as such the no scan was carried out. As it can be seen on sample A, in which was applied a load of 1200 N demonstrates a small damage area on the reinforcement. The non-destructive test (NDT) using DolphiCam2$^{TM}$ computed the damaged the area to be 145.69 $mm^2$ with are circumference of 42.79 mm and a diameter of 13.62 mm.

In pressure vessel B, using an impact loading of 2200 N caused a damaged of $90^0$ fibre orientation showing fibre break. Then in sample C and D, an applied load of 3200 N and 4200 N, respectively, resulted in delamination and cracking of the matrix and fibre failure.

### 4.2. Compression strength

The compressive strength of the spacemen is calculated by $\sigma_c = \frac{F_{max}}{\pi(r_o^2 - r_i^2)}$ where $F_{max}$- maximum applied force, $r_o$ -outer radius and $r_i$- inner radius. The damage is expected to occur around the middle of the surface of the cylinders subjected to quasi-static damage. The failure at the end of the cylinder can occur before the real compression of the cylinder is achieved. Composite cylinders were tested to characterise its compressive strength performance. In this section, the axial compression of the damaged and non-damaged cylinders is analysed. The main objective is to analyse the change in the compressive strength of the pressure vessels after being damaged.

The outcome of the experiment for all damaged and non-damaged pressure vessels are remarkably similar. However, when the cylinders are subjected to quasi-static compression, the polyethylene absorbs enough elastic strain energy to recover from the applied compressive load and recover without being plastically deformed.

During the experiment, it was possible to hear the fibre cracking while compressing; consequently, the noise of the fibre breaking under compression as demonstrates in Fig. 21 as the first failure. Therefore, the first break might be a separation between the filament winding and the polyethylene from the bottom to the top or opposite. Thus, as the cylinder is compressed it starts to absorb more load, because the polyethylene kept resisting the compression as a separate material. Nevertheless, the buckle of the inner cylinder occurs, and the composite cylinder fails. Therefore, the failure modes observed at the bottom of the cylinders are brooming and local buckling.

Moreover, the stress–strain curve is presented in Fig. 22, for the different cylinders, showing how it breaks initially and because it presents similar failure to buckling it buckles and then supports stress until loading is ceased or removed.

In addition, 4200 N load is applied to achieve penetration through the pressure vessel which correlated with previous studies on the damage reported including surface breaking, delamination, matrix cracks and fibre breakage, being at the point where the material actually fractures Shyr and Pan [34]. Moreover, looking at the energy absorbed is shown that with the increase of the deflection the more energy is absorbed by the specimen in the quasi-static compression test, this phenomenon is also observed on studies by Kobayashi and Kawahara [22] and by Rydr and Black [35] noting that the stiffness of the CFRP is improved if the vessels thickness is increased; similarly, this proved to have reduced the plastic deformation by indentation. However, the damage to the vessels during impact might provide a linear response, then shifting to non-linear, due to the cylinder starting to deform. The effect of acceleration drop indicates the composite failure and the reduction of material resistance to impact as established by Mouti et al. [23] and Duell [36].

## 5. Conclusions

In this study, composite cylinders were tested to characterise their compressive strength performance and load bearing capacities by experimental procedures with quasi-static compression testing and axial compression testing. In quasi-static compression testing, the cylinders were damaged at the centre with set peak loads of 1200 N, 2200 N, 3200 N and 4200 N. The results showed that the damage from the quasi-static compression test does not influence on the compressive strength of the

cylinders under axial compression. Additionally, all the samples failed at the same location (bottom neck); consequently, the failure can be characterised as fibre break, delamination, brooming and local buckling failure. Fibres are the main load-bearing element in the pressure vessel, the decrease in burst pressure is mainly established by the degree of fibre damages. Burst pressure of the damaged pressure vessels lowered with a rise in the axial level of observable fibre damage. The examinations revealed that burst pressure of the vessel is significantly affected only when a visually evident fibre split (micro-buckling) is present.

The quasi-static compression testing was performed with set applied loads at the centre of the pressure vessel, the results show that the absorbed energy from the cylinders increased as the load was applied resulting in high deformation. The deformation was analysed in the elastic region of the composite. Then, axial compression testing of damaged and non-damaged cylinder shows that previous damaged form quasi-static compression does not affect the compression strength of the composite cylinder when subjected to axial compression. So, all the tested cylinders buckled at the bottom neck. Fibre damage generated by compression appeared slightly away from the impact region. The failure mechanism involves outer layer fibres peel off and fibre debonding where fibre damage had previously been inflicted. The residual burst strength of the cylindrical composite overwrapped pressure vessels critically depends on the fibre damage in the hoop layers.

Microscopy and non-destructive tests characterised the damaged establishing the extent of the damage in terms of area, circumference and penetration depth. Moreover, microscopy established fibre cracking, breakage and debonding resulting from the quasi-static loads applied. Matrix cracks generally propagated to end up being delamination's because of the difference of the fibre orientation between layers, and also the delamination's critically lowered the bending rigidity of the structures. A tiny disparity of the fibre direction in the hoop layers generated the delamination in the group of hoop layers. Fibre damage generated by compression appeared slightly away from the impact region. The failure mechanism involves outer layer fibres peel off and fibre debonding where fibre damage had previously been inflicted. The residual burst strength of the cylindrical composite overwrapped pressure vessels critically depends on the fibre damage in the hoop layers. The results for the damage profile and the effect on compressive strength of the composite damaged and two non-damaged cylinders was found to be relatively similar. Additionally, the results demonstrate that the quasi-static compression have little or no influence on the axial strength of the cylinders. This new remarkable finding on performance of composite pressure vessel under damaged and undamaged conditions has established the reliability and load bearing capacities and strength capabilities of composites under the scenarios investigated.

## CRediT authorship contribution statement

**Auwalu I. Mohammed:** Conceptualization, Methodology, Formal analysis, Investigation, Data curation, Writing – original draft, Writing – review & editing, Visualization. **Kaarthikeyan Raghupathy:** Conceptualization, Methodology, Formal analysis, Investigation, Data curation, Writing – original draft, Writing – review & editing, Visualization. **Osvaldo De Victoria Garcia Baltazar:** Conceptualization, Methodology, Formal analysis, Investigation, Data curation, Writing – original draft, Writing – review & editing, Visualization. **Lawson Onokpasah:** Conceptualization, Methodology, Formal analysis, Investigation, Data curation, Writing – original draft, Writing – review & editing, Visualization. **Roger Carvalho:** Methodology, Formal analysis, Investigation, Data curation, Writing – original draft, Writing – review & editing, Visualization. **Anders Mogensen:** Methodology, Formal analysis, Investigation, Data curation, Writing – original draft, Writing – review & editing, Visualization. **Farzaneh Hassani:** Methodology, Formal analysis, Investigation, Data curation, Writing – original draft, Writing – review & editing, Visualization. **James Njuguna:** Conceptualization, Methodology, Formal analysis, Investigation, Resources, Data curation, Writing – original draft, Writing – review & editing, Visualization, Supervision, Project administration, Funding acquisition.

## Declaration of Competing Interest

The authors declare that they have no known competing financial interests or personal relationships that could have appeared to influence the work reported in this paper.

## Data availability

Data will be made available on request.

## Acknowledgment

The authors would like to acknowledge Mr Allan MacPherson, Mr Alexander Laing and Mr David Smith for their technical support during testing and helpful discussions to this study. This research was partly funded by the Scottish Government Emerging Energy Transition Fund, Hydrogen Innovation Scheme, Stream 2 (Project No. EETF/HIS/ APP/ 007).

## References

[1] McLaughlan PB, Forth SC, Grimes-Ledesma LR 2011. *Composite overwrapped pressure vessels, a primer* (No. S-1046).
[2] Rafiee R, Torabi MA. Stochastic prediction of burst pressure in composite pressure vessels. Compos Struct 2018;185:573–83.
[3] Slattery PG, McCarthy CT, O'Higgins RM. Assessment of residual strength of repaired solid laminate composite materials through mechanical testing. Compos Struct 2016;147:122–30.
[4] Kangal S, Kartav O, Tanoğlu M, Aktaş E, Artem HS. Investigation of interlayer hybridization effect on burst pressure performance of composite overwrapped pressure vessels with load-sharing metallic liner. J Compos Mater 2020;54(7):961–80.
[5] Wu Q, Chen X, Fan Z, Jiang Y, Nie D. Experimental and numerical studies of impact on filament-wound composite cylinder. *Acta mechanica solida sinica* 2017;30(5):540–9.
[6] Perillo G, Grytten F, Sørbø S, Delhaye V. Numerical/experimental impact events on filament wound composite pressure vessel. Compos B Eng 2015;69:406–17.
[7] Blanc-Vannet P. Burst pressure reduction of various thermoset composite pressure vessels after impact on the cylindrical part. Compos Struct 2017;160:706–11.
[8] Zhang X, Bianchi F, Liu H. Predicting low-velocity impact damage in composites by a quasi-static load model with cohesive interface elements. Aeronaut J 2012;116(1186):1367–81.
[9] Rafiee R, Ghorbanhosseini A, Rezaee S. Theoretical and numerical analyses of composite cylinders subjected to the low velocity impact. Compos Struct 2019;226:111230.
[10] Rafiee R, Rashedi H, Rezaee S. Theoretical study of failure in composite pressure vessels subjected to low-velocity impact and internal pressure. Front Struct Civ Eng 2020;14:1349–58.
[11] AZOM, 2001. *E-Glass Fibre*. [online]. AZoM.com. Available from: https://www.azom.com/article.aspx?ArticleID=764 [Accessed 16 April 2022].
[12] IONEOS, 2017. *Typical Engineering Properties of High Density Polyethylene* [PDF]. [online]. League City, Teas: Ioneos. Available from: https://www.ineos.com/globalassets/ineos-group/businesses/ineos-olefins-and-polymers-usa/products/technical-information–patents/ineos-typical-engineering-properties-of-hdpe.pdf [Accessed 16 April 2022].
[13] Benham PP, Crawford RJ, Armstrong CG. Mechanics of engineering materials. Harlow Longman Group; 1996.
[14] Sachse S, Poruri M, Silva F, Michalowski S, Pielichowski K, Njuguna J. Effect of nanofillers on low energy impact performance of sandwich structures with nanoreinforced polyurethane foam cores. J Sandw Struct Mater 2014;16(2):173–94.
[15] Sutherland LS, Soares CG. The use of quasi-static testing to obtain the low-velocity impact damage resistance of marine GRP laminates. Compos B Eng 2012;43(3):1459–67.
[16] Krishnaswamy RK. Analysis of ductile and brittle failures from creep rupture testing of high-density polyethylene (HDPE) pipes. Polymer 2005;46(25):11664–72.
[17] Curtis J, Hinton MJ, Li S, Reid SR, Soden PD. Damage, deformation and residual burst strength of filament-wound composite tubes subjected to impact or quasi-static indentation. Compos B Eng 2000;31(5):419–33.
[18] Korsunsky AM. Elastic behavior of materials: continuum aspects. *Encyclopedia of Materials: Science and Technology*; 2011 pp.2398-2404.
[19] Weirdie BL, Lagace PA. On the use of quasi-static testing to assess impact damage resistance of composite shell structures. Mech Compos Mater Struct Int J 1998;5(1):103–19.

[20] Liu L, Xu W. Effects of fillers on the impact damage and compressive residual properties of single hat-stiffened composite panels. Thin-Walled Struct 2022;180:109705.
[21] Karakuzu R. "An experimental investigation of the impact response of composite laminates," vol. 87, pp. 307–313, 2009, doi: 10.1016/j.compstruct.2008.02.003.
[22] Kobayashi S, Kawahara M. Effects of stacking thickness on the damage behavior in CFRP composite cylinders subjected to out-of-plane loading. Compos A Appl Sci Manuf 2012;43(1):231–7.
[23] Mouti Z, Westwood K, Long D, Njuguna J. Finite Element Analysis of Glass Fiber-Reinforced Polyamide Engine Oil Pan Subjected to Localized Low Velocity Impact from Flying Projectiles. Steel Res Int 2012;83(10):957–63.
[24] Weaver PM. Design of laminated composite cylindrical shells under axial compression. Compos B Eng 2000;31(8):669–79.
[25] Njuguna J. ed., 2016. Lightweight composite structures in transport: design, manufacturing, analysis, and performance. Woodhead publishing.
[26] Kim EH, Lee I, Hwang TK. "Impact response and damage analysis of composite overwrapped pressure vessels," *Collect. Tech. Pap. - AIAA/ASME/ASCE/AHS/ASC Struct. Struct. Dyn. Mater. Conf.*, no. April, pp. 1–7, 2011, doi: 10.2514/6.2011-1863.
[27] Banik A, Zhang C, Khan MH, Wilson M, Tan KT. Low-velocity ice impact response and damage phenomena on steel and CFRP sandwich composite. Int J Impact Eng 2022;162:104134.
[28] Tuo H, Wu T, Lu Z, Ma X, Wang B. Study of impact damage on composite laminates induced by strip impactor using DIC and infrared thermography. Thin-Walled Struct 2022;176:109288.
[29] Njuguna J, Michałowski S, Pielichowski K, Kayvantash K, Walton AC. Fabrication, characterization and low-velocity impact testing of hybrid sandwich composites with polyurethane/layered silicate foam cores. Polym Compos 2011;32(1):6–13.
[30] Pattarakunnan K, Galos J, Das R, Mouritz AP. Impact damage tolerance of energy storage composite structures containing lithium-ion polymer batteries. Compos Struct 2021;267:113845.
[31] Reynolds J, Ali D, Njuguna J. The state of the art in hydrogen storage. Green Energ. Ennvironm. 2023 https://rgu-repository.worktribe.com/output/2079419.
[32] Allen T, Ahmed S, Hepples W, Reed PA, Sinclair I, Spearing M. A comparison of quasi-static indentation and low-velocity impact on composite overwrapped pressure vessels. J Compos Mater 2018;52(29):4051–60.
[33] Barral K, Barthélémy H. Hydrogen high pressure pressure vessels storages: overview and new trends due to H2 Energy specifications and constraints; 2006. *June. http://www. cder. dz/A2H2/Medias/Download/Proc% 20PDF/PARALLEL% 20SESSIONS/[S12], 20.*
[34] Shyr TW, Pan YH. Impact resistance and damage characteristics of composite laminates. Compos Struct 2003;62(2):193–203.
[35] Ryder JT, Black ED. Compression testing of large gage length composite coupons. In *Composite Materials: Testing and Design (Fourth Conference); Davis, JG, Ed* (pp. 170-189); 1974.
[36] Duell JM. Impact testing of advanced composites. *Advanced topics in characterization of composites*, 2004;*97*, pp.97-112.

## *Further reading*

[37] Nguyen DH, Kim JH, Vo TTN, Kim N, Ahn HS. Design of portable hydrogen pressure vessel using adsorption material as storage media: An alternative to Type IV compressed pressure vessel. Appl Energy 2022;310:118552.
[38] Maus S, Hapke J, Ranong CN, Wüchner E, Friedlmeier G, Wenger D. Filling procedure for vehicles with compressed hydrogen pressure vessels. Int J Hydrogen Energy 2008;33(17):4612–21.